

Failure analysis of seven masonry churches severely damaged during the 2012 Emilia-Romagna (Italy) earthquake: Non-linear dynamic analyses vs conventional static approaches

Gabriele Milani*, Marco Valente

Department of Architecture, Built Environment & Construction Engineering ABC, Politecnico di Milano, Piazza Leonardo da Vinci 32, 20133 Milan, Italy

Received 28 December 2014

Received in revised form 8 March 2015

Accepted 24 March 2015

Available online 31 March 2015

1. Introduction

It is estimated there are more than 64,000 churches in Italy. The majority is classified into the group of “monumental historical structures”, is masonry construction and is located in high-seismicity regions. It has been recently calculated that, after the devastating 5.9 and 5.8 magnitude earthquakes occurred in Emilia-Romagna respectively on 20th and 29th of May 2012, the churches considered unsafe – i.e. with an induced level of damage that prevents their utilization – have been more than 500 only in the provinces of Modena, Ferrara and Bologna. After more than two years from the seismic sequence, a

* Corresponding author. Tel.: +39 022399 4290; fax: +39 022399 4220.

E-mail address: gabriele.milani@polimi.it (G. Milani).

great part of the damaged churches is still awaiting for seismic rehabilitation and suitable strengthening to improve their performance under horizontal loads.

As well known, churches are not conceived to properly withstand earthquakes [1–11] and post-seismic surveys have demonstrated that the activation of partial collapses [12] is critical even at very low levels of horizontal acceleration. High and slender perimeter walls scarcely interconnected, long and wide naves carried by slender columns, quite poor masonry quality and presence of flexible wooden roofs [13–17] promote the activation of mechanisms involving few macro-blocks into local failures [18–27].

Unfortunately, churches cannot be reduced to any standard static scheme [18–27]. Italian Guidelines for the Cultural Heritage [28] help practitioners in the safety assessment. To evaluate the acceleration at collapse, they suggest a quite rough and conventional approach based on pre-assigned partial failure mechanisms and the utilization of the kinematic theorem of limit analysis within the assumption of a no-tension material model for masonry. An abacus of twenty-eight possible collapse mechanisms, based on experience of failures observed during past earthquakes, is provided.

Despite the simplicity of such an approach, however, some drawbacks are quite evident, as for instance the risk to overestimate the horizontal acceleration at failure due to the identifications of wrong failure mechanisms and the rough simplifications introduced in the actual geometry of the case under study.

To overcome such limitations, a FE upper bound limit analysis procedure has been recently applied successfully by one of the authors of this paper on a variety of different examples, including many churches in seismic regions [18–20].

An alternative to limit analysis, which however still remains scarcely available in commercial codes (even if some exceptions, basically conceived for either geotechnical problems [29] or specialized to masonry arches [30], are present in the literature), is represented by pushover analysis. Italian Guidelines on the Built Heritage [28] implicitly state that the equivalent frame approximation cannot be used for existing buildings with peculiar geometries, as for instance castles, churches and towers, but at the same time suggest to perform a conventional static analysis also with simplified materials where softening is not included. As well known, indeed, non-linear static analyses, conducted when the global behavior beyond the maximum load carrying capacity is required, cannot be easily obtained using refined FE discretizations with many 2D and 3D elements, as needed for a realistic analysis of masonry churches. In addition, complex material models are not generally implemented in the majority of the commercial codes available for standard design. Several commercial software packages usually put at disposal elastic-perfectly plastic models, with isotropic behavior, friction (either Mohr–Coulomb or Drucker–Prager strength domains) and associated flow rule.

In this context, it appears rather clear that, despite the level of complexity of the FE analysis which still remains almost prohibitive for a great part of the involved practitioners, the limits of applicability of a non-linear static approach should be deeply investigated and considered with care.

One of the main purposes of the paper is to quantitatively analyze if the utilization of simplified material models for masonry and the application of horizontal loads according to static approaches are anyway acceptable and, if so, what is the level of accuracy and approximation of the results obtained.

To validate the effectiveness of such simplified procedures, as suggested by Italian Code, in the present paper time-consuming non-linear dynamic analyses are performed, using detailed FE discretizations of the same seven churches analyzed in [11]. An isotropic non-linear material exhibiting softening and damage, frictional behavior and different strength in tension and compression is used for masonry.

The present numerical investigations may therefore be regarded as the natural sequel of previously presented [11] static and simplified approaches, where the novelty is represented by the application of non-linear dynamic analyses to quite complex geometries. Attention is mainly focused on the role played by the geometric variability (especially in plan) of the different case studies analyzed, with particular regard to geometric irregularities and interlocking between perpendicular walls.

Furthermore, it is emphasized that 14 non-linear dynamic analyses (carried out applying the same accelerogram, separately, along the longitudinal and transversal directions for each church) are performed on rather demanding FE models, each one requiring up to 6 days to be processed on workstations equipped with large RAM. While such computational effort is obviously impossible to manage in common design, the study should be regarded as a reference in the field, because it puts in evidence – by means of the sensitivity analysis conducted discussing the role played by the different geometries – how effective can be a simplified approach based on the a-priori assumption of a given failure mechanism or a standard elastic response spectrum procedure.

Kinematic FE limit analyses predictions (which provide similar results to the ones obtained by FE 3D pushover approaches, as demonstrated in [11]) are systematically compared with non-linear dynamic analyses performed on the aforementioned seven masonry churches, exhibiting different geometrical features. Detailed comparisons among the active failure mechanisms provided by both limit analysis and FE non-linear dynamic approach are reported. It is found that, in the majority of the cases, the active failure mechanism is identified correctly, but that the results (e.g. collapse acceleration, behavior factor) are affected by a level of approximation that may considerably depend on in-plan irregularity and hypotheses done on the interlocking between contiguous walls. From a quantitative point of view, a non-linear dynamic analysis is able to provide – among other information – residual displacements of the control nodes. By using these data, practitioners should decide, on the basis of their own experience or consolidated models, if such values are compatible or not with the equilibrium condition of the macro-block where the failure mechanism is acting. If not, it means the accelerogram applied causes a partial failure of the structure. It is also interesting to investigate, as done in this paper, such a result is in agreement with what provided by a standard eigen-frequency analysis associated with the response spectrum related to the applied

accelerogram, i.e. if spectral accelerations exhibit peaks near the periods of the structures associated with the highest percentage of participating mass. The results found are in relatively good agreement for all the cases examined, once again confirming that the right way to proceed in practice is represented by the utilization of many different approaches, ranging from

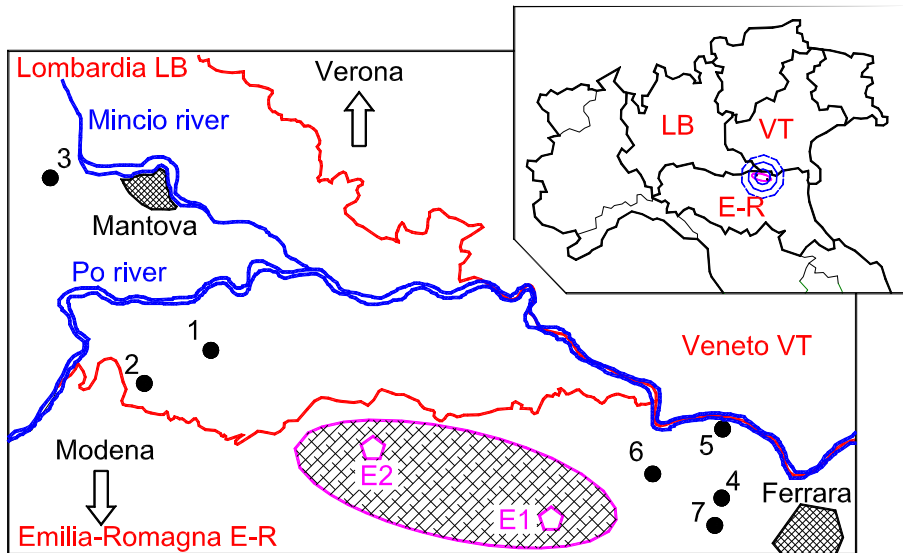


Fig. 1. Location of the churches under study (E1 and E2 approximately represent the epicenters of M 5.9 and M 5.8 seismic events, respectively).

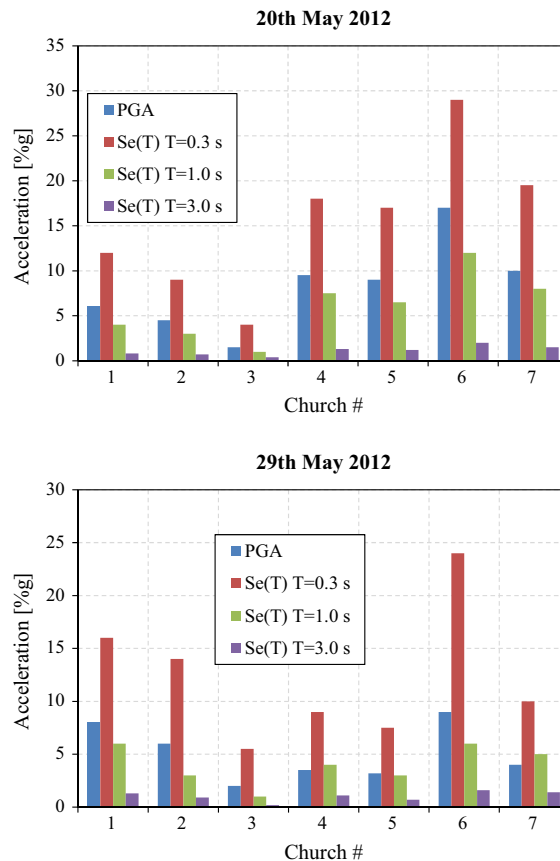


Fig. 2. PGA and spectral accelerations (for three vibration periods of a single-DOF elastic system), 20th and 29th May 2012 seismic events.

standard eigen-frequency analyses, passing through pushover and limit analyses with no-tension materials, and ending with non-linear dynamic procedures. The effectiveness of the use of different approaches (non-linear static and dynamic analyses) for seismic performance assessment of other typologies of structures is described in [31–34].

2. Modeling strategies and brief description of the case studies analyzed

The case studies used to compare the different analysis procedures proposed by Italian Code are represented by seven masonry churches located near the two epicenters of the major seismic events, see Fig. 1. Most of these churches have been severely damaged and have been closed because considered unsafe. The peak ground accelerations (PGA) estimated for the seven churches under consideration are reported in Fig. 2, where spectral accelerations are also represented for three vibration periods of a single-DOF system, equal to 0.3, 1.0 and 3.0 s, respectively. The reader interested in a very detailed analysis of the seismic sequence from a seismologic point of view is referred to [35–37]. Here, the aim is only to highlight that an amplification of the spectral acceleration is always present for structures with fundamental period equal to 0.3 s. From experience of the authors in the field, the fundamental vibration mode involving a significant percentage of participating



Fig. 3. Lateral and front views of Churches 1–4 and 3D FE discretization.

mass provided by a standard eigen-frequency analysis is typically near 0.3–0.4 s for churches. As a consequence, such structures experienced the highest amplifications of PGAs. These features could partially justify the damage to the churches caused by the seismic sequence.

The FE discretizations along with a rough indication of the dimensions of the analyzed churches are shown in Fig. 3 for Churches 1–4 and in Fig. 4 for Churches 5–7. All the plan views with a rough indication of the dimensions of the churches are reported in Fig. 5. The reader interested in a detailed description of the geometry and in a survey of the damages observed after the seismic events is referred to [11].

Generally, when dealing with masonry geometry and mechanical properties (brick pattern, thickness and through-thickness behavior), it is possible to conclude that all the structures exhibit similar features. In particular, the thickness of the load bearing walls ranges between 40 and 100 cm. Masonry is a multi-head one and is constituted by relatively high resistance clay bricks, brick pattern is regular, with joints thickness approximately equal to 10 mm. Mechanical properties adopted in this study are in agreement with Italian Code [38,39] specifics and will be discussed later in the paper. Hereafter, only a concise description of the main geometrical features of the churches is provided.

- Church 1, San Giacomo Maggiore Apostolo in Pegognaga, is a single nave structure with small lateral chapels. It is approximately 29 m long, with a 9.30 m wide and 18 m long nave. The presbytery is rectangular, 5.80 m long, and ends with a circular apse. There are four chapels, two per side, 1.80 m large and 4.75 m long. A light timber roof covers the nave.
- Church 2, San Sisto II in Palidano di Gonzaga, has a single nave approximately 23 m long. The façade, 22 m high, exhibits a curved shape. The nave is flanked by two chapels on either side and the apse is circular, with height equal to 13.50 m. The presbytery is rectangular, 8 m long. The inclined bell tower, survived the demolition of an old church, results incorporated into the new building. Some rectangular masonry columns (section equal to 80 × 60 cm), built in adhesion to perimeter walls, better diffuse vertical loads transferred by the roof.
- Church 3, San Giorgio Martire in Castellucchio, has a Greek cross plan, 31.5 m long, with four internal large columns carrying a non-structural central vault. The intersection of the naves with the transept architecturally defines five distinct zones with different heights: the central vault reaches a height equal to 15.7 m, while the four lateral zones are 8 m high. The thickness of the external walls is equal to 60 cm. The façade is a typically Romanesque one and has a thickness equal to 70 cm.

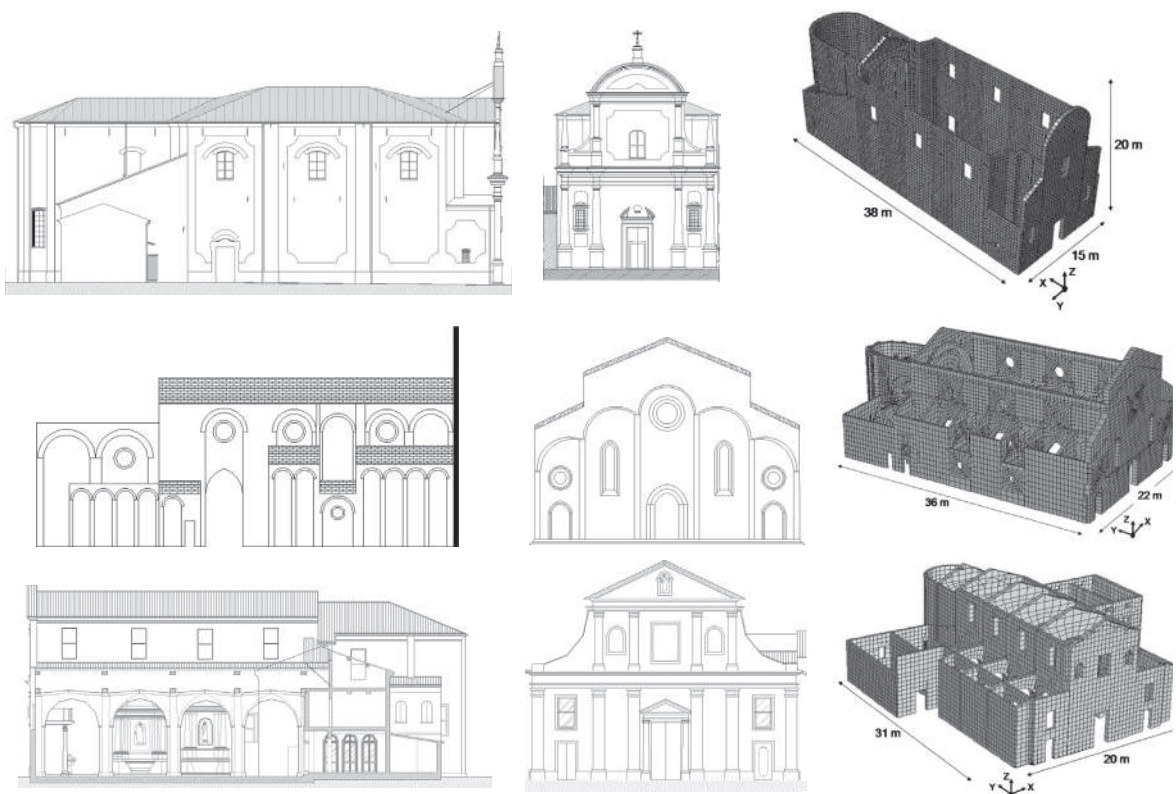


Fig. 4. Lateral and front views of Churches 5–7 and 3D FE discretization.

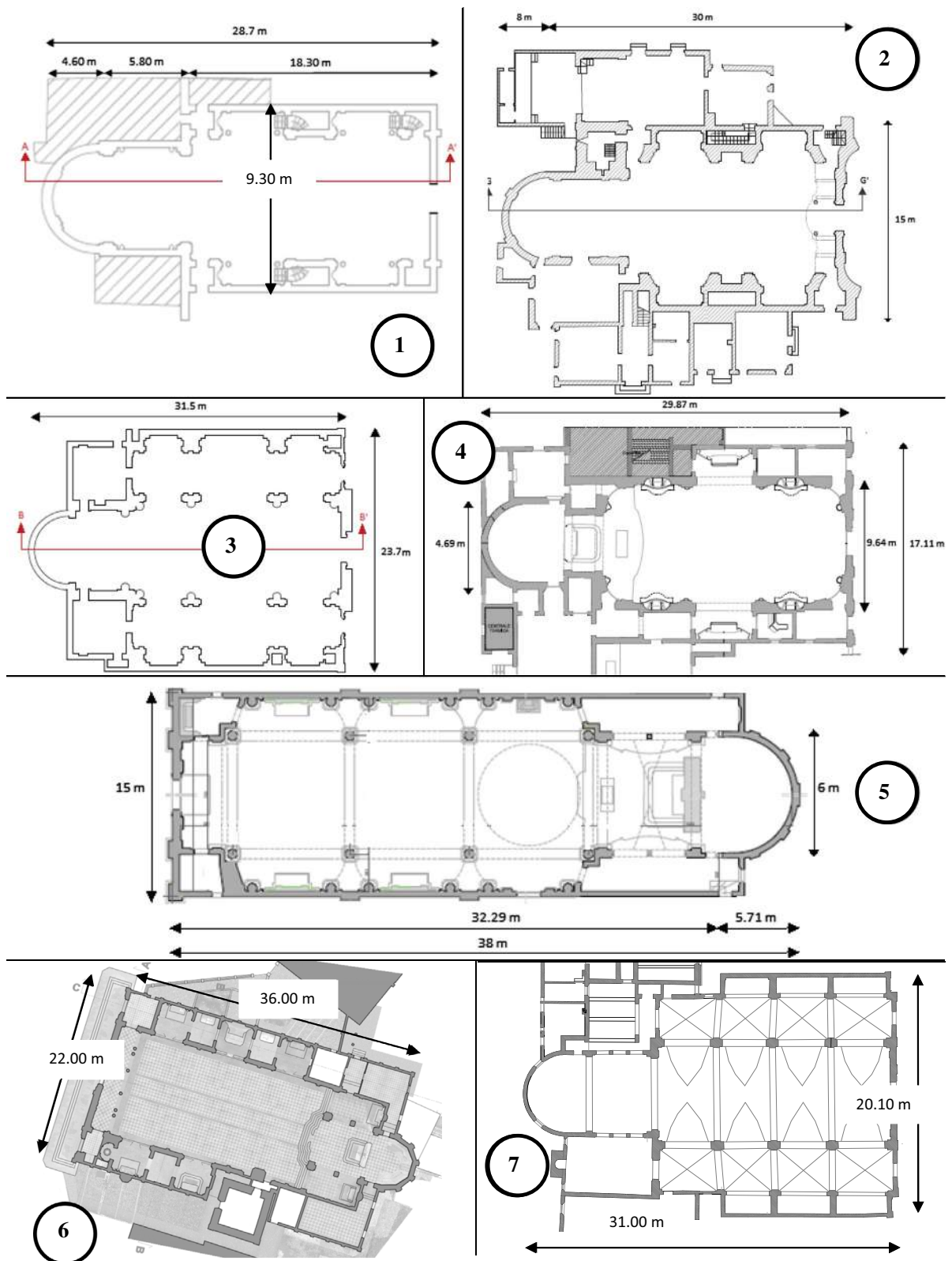


Fig. 5. Plan views of the churches under study with rough indication of the dimensions.

- Church 4, Santi Pietro e Paolo in Vigarano Pieve, is a single nave structure with dimensions in plan approximately equal to 30×17 m. Some small chapels are attached laterally. The presbytery is 4.70 m wide, ends with a circular apse and has a length approximately equal to 10 m. The height of the lateral walls is equal to 11.20 m and decreases up to 8.10 m in correspondence of the presbytery. The façade is 18.30 m high and 17.1 m wide.
- Church 5, Santi Filippo e Giacomo in Ravalle (Fig. 4), has a very long presbytery (15 m), not particularly large (6 m), and a quite wide single central nave. The apse is circular. There are three quite large windows on the lateral walls. The façade is about 20 m high, with a tympanum not interconnected with perpendicular walls. Some tires were installed about one century ago to partially preclude the overturning of the tympanum.
- Church 6, Natività di Maria Vergine in Bondeno (Fig. 4), is a single nave structure with continuous lateral chapels, approximately 36 m long and 22 m wide. The façade, 19 m high, is built with a typical Romanesque style. The apse and the bell tower date back to the Middle Age (1200), whereas the majority of the church was re-built in the 1870–1890 decades. The bell tower is almost totally isolated from the church, exception made for a very small corridor of interconnection at the ground floor level. For this reason, it is not taken into consideration in the model.
- Church 7, Natività della Beata Maria Vergine in Vigarano Mainarda (Fig. 4), is constituted by three naves, with dimensions approximately equal to $21 \text{ m} \times 20 \text{ m} \times 13 \text{ m}$ (length \times width \times maximum height). Five transversal arches interconnect the lateral walls to the central nave, thus making the behavior of the church more global. The façade is poorly interconnected with perpendicular walls. The church is laterally connected to a secondary sacristy on the left and to a large oratory on the right; only parts of them are considered in the FE discretization to simplify the analyses.

3. Non-linear dynamic analyses

In order to capture all possible failure mechanisms, non-linear dynamic analyses should be performed by applying an acceleration time-history, defined by a natural or artificial record, at the base of the structure. Such method of analysis may be time-consuming in practical applications for the analysis of the inelastic behavior of large structures, but it is much

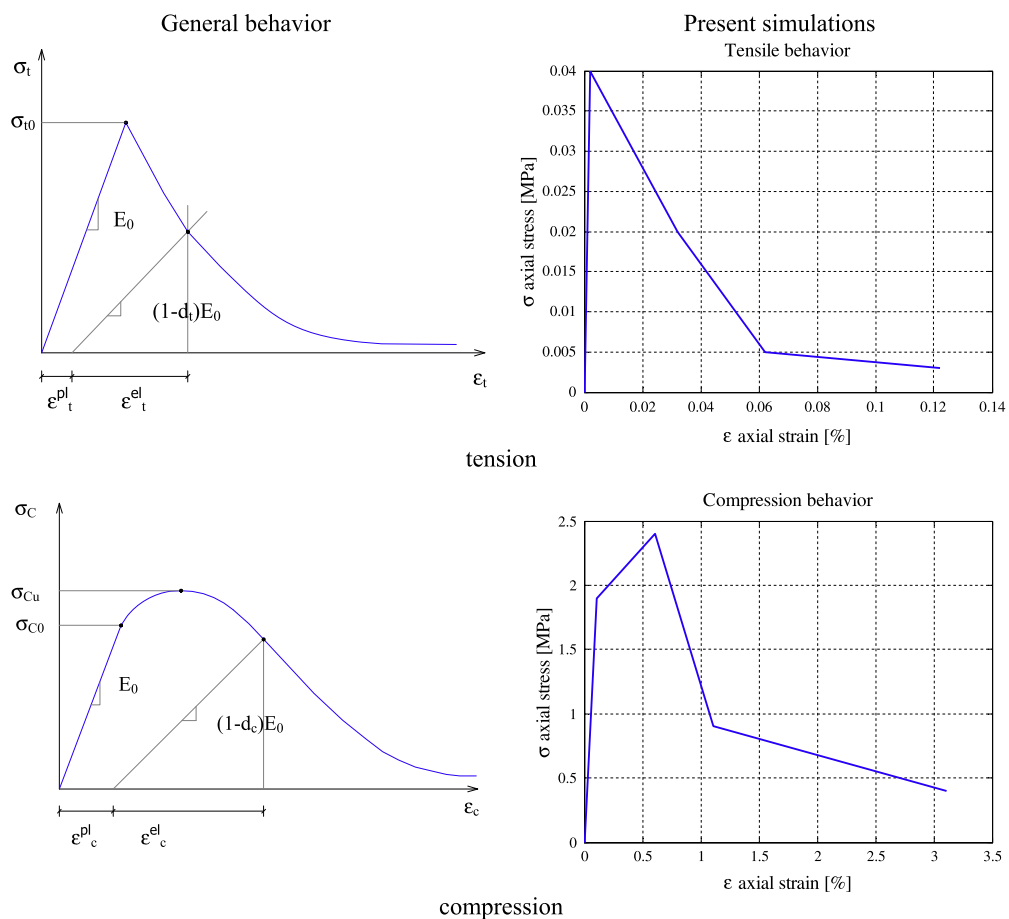


Fig. 6. Non-linear uniaxial stress-strain behavior in tension (top) and compression (bottom) adopted in the simulations (left: general ABAQUS model; right: actual multi-linear behavior utilized).

more accurate and reliable than other approaches for its capability to identify in- and out-of-plane, as well as local and global failure mechanisms. For this reason, in this study it is used to validate the static approaches employed in common practice and, in case, to highlight their limits of applicability.

Based on such information, the three-dimensional finite element models of the churches under study are implemented in Abaqus [40], taking into consideration geometrical (large displacement effects) and material non-linearity (elastic-plastic with damaging behavior of the masonry material), with the aim of investigating their seismic response by means of non-linear dynamic analyses.

The use of sophisticated 3D models requires a relatively reasonable computational effort on sufficiently powerful workstations (4–6 days for a single dynamic simulation), if the discretizations are not excessively refined and the material models do not exhibit strong softening.

On the other hand, Italian Guidelines for the Built Heritage [28] specify that such analyses can be conducted using finite element models and considering suitable constitutive models. Such models should be capable of reproducing the typical strength and stiffness degradation exhibited by the masonry material in the inelastic range.

Italian Code on Constructions NTC 2008 [38] and subsequent explicative notes [39] underline that the aim of dynamic analyses would be the evaluation of the behavior of the structure in the non-linear range under an expected accelerogram, providing a comparison between required and available ductility. Also, it is possible to verify the integrity of the structural elements which can potentially show brittle behavior. The use of a minimum of three different accelerograms compatible with the response spectrum is recommended by Italian Guidelines [28].

In this study, the structures were subjected to the same real accelerogram, recorded at Mirandola Station on the 20th of May 2012 (first shake). The reason is mainly linked to the fact that the churches analyzed are located in different positions and, therefore, the response spectra to be used would be different. To make the results comparable, it was therefore needed to apply the same accelerogram to all the structures.

When dealing with material properties assumed and available in FE Abaqus code, the so-called “Concrete Damage Plasticity” model was adopted [41]. Such a model is based on the assumption of a scalar isotropic damage with distinct damage parameters in tension and compression. It is particularly suitable for applications in which the material exhibits damage, especially under load-unload conditions and hence for dynamic analyses. An elastic-plastic behavior in both tension and compression can be also taken into account, as illustrated in Fig. 6.

To describe the multi-dimensional behavior in the inelastic range, masonry is assumed obeying a Drucker-Prager strength criterion with non-associated flow rule, Fig. 7. A value equal to 10° is adopted for the dilatation angle, which seems reasonable for a masonry material subjected to moderate-low levels of vertical compression, also in agreement with experimental evidences available in the literature, see e.g. [42,43]. To avoid numerical convergence issues, the tip of the conical

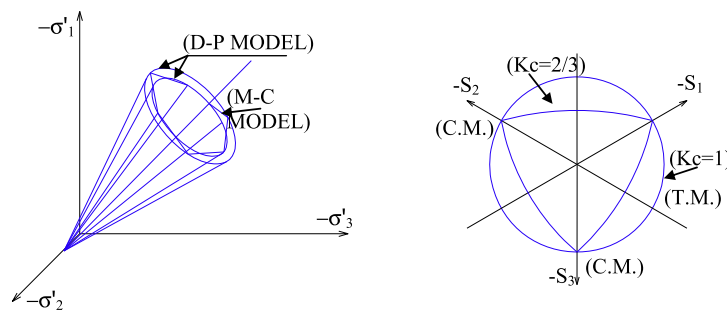


Fig. 7. Left: 3D strength domain adopted in the dynamic simulations, principal stresses space (D-P: Drucker-Prager failure criterion; M-C: Mohr-Coulomb failure criterion). Right: K_c parameter to approximate with a D-P failure criterion a M-C failure criterion in a smooth way.

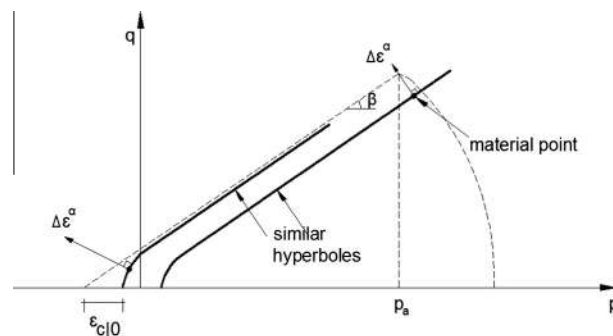


Fig. 8. Smoothed Drucker-Prager failure criterion adopted in the simulations, p - q plane.

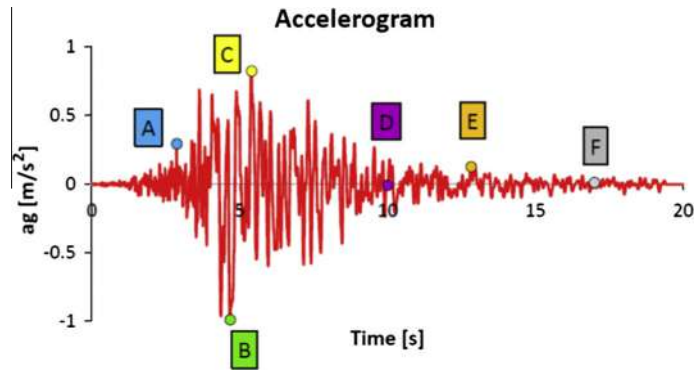


Fig. 9. Scaled real accelerogram used in the dynamic analyses and meaningful points used to evaluate the damage state of the churches under study.

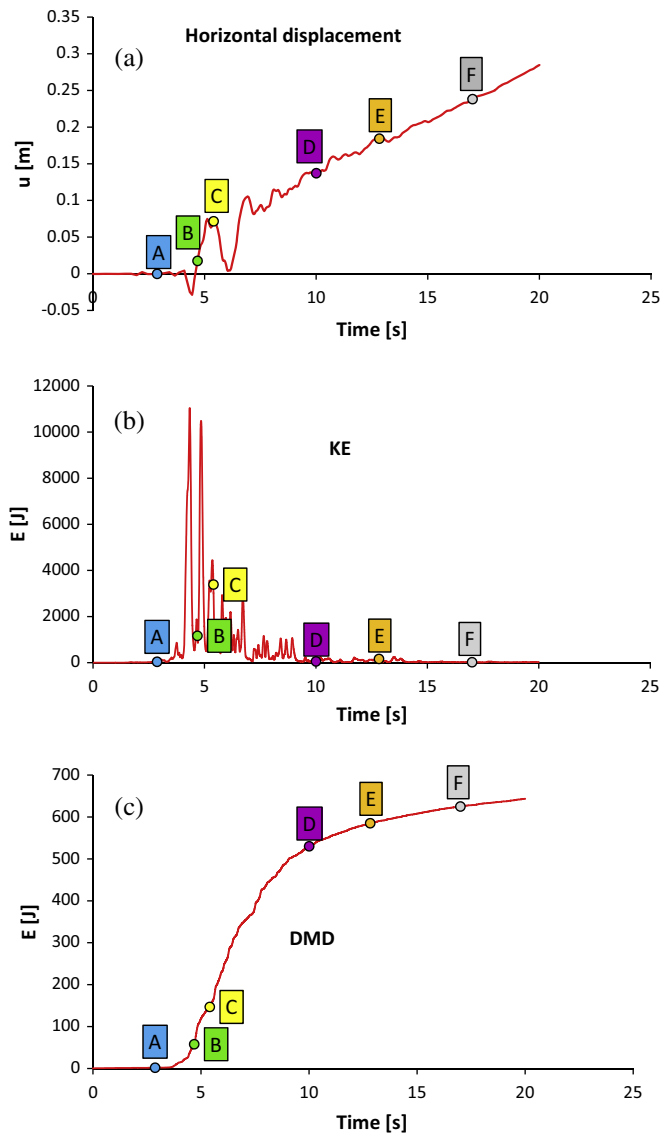


Fig. 10. Church 1. Seismic excitation in the longitudinal direction of the church. (a) Control point horizontal displacement time-history diagram. (b) Kinetic energy time-history diagram. (c) Energy dissipation in tension time-history diagram.

domain of the Drucker–Prager strength domain is smoothed with a function having hyperbolic shape. Abaqus code allows ruling smoothing by means of the so-called eccentricity parameter, which represents the length of the segment between the points of intersection of the cone and of the hyperbola with the p axis in the p – q space, see Fig. 8. A value equal to 0.1 is adopted for the eccentricity parameter.

Experimental results reported by Page on regular masonry wallets [44] and successive numerical models [45,46] show that such a material exhibits a moderate orthotropy ratio (around 1.2) under biaxial stress states in the compression–compression region. Obviously, such a feature cannot be taken into account when an isotropic model, like the present one, is

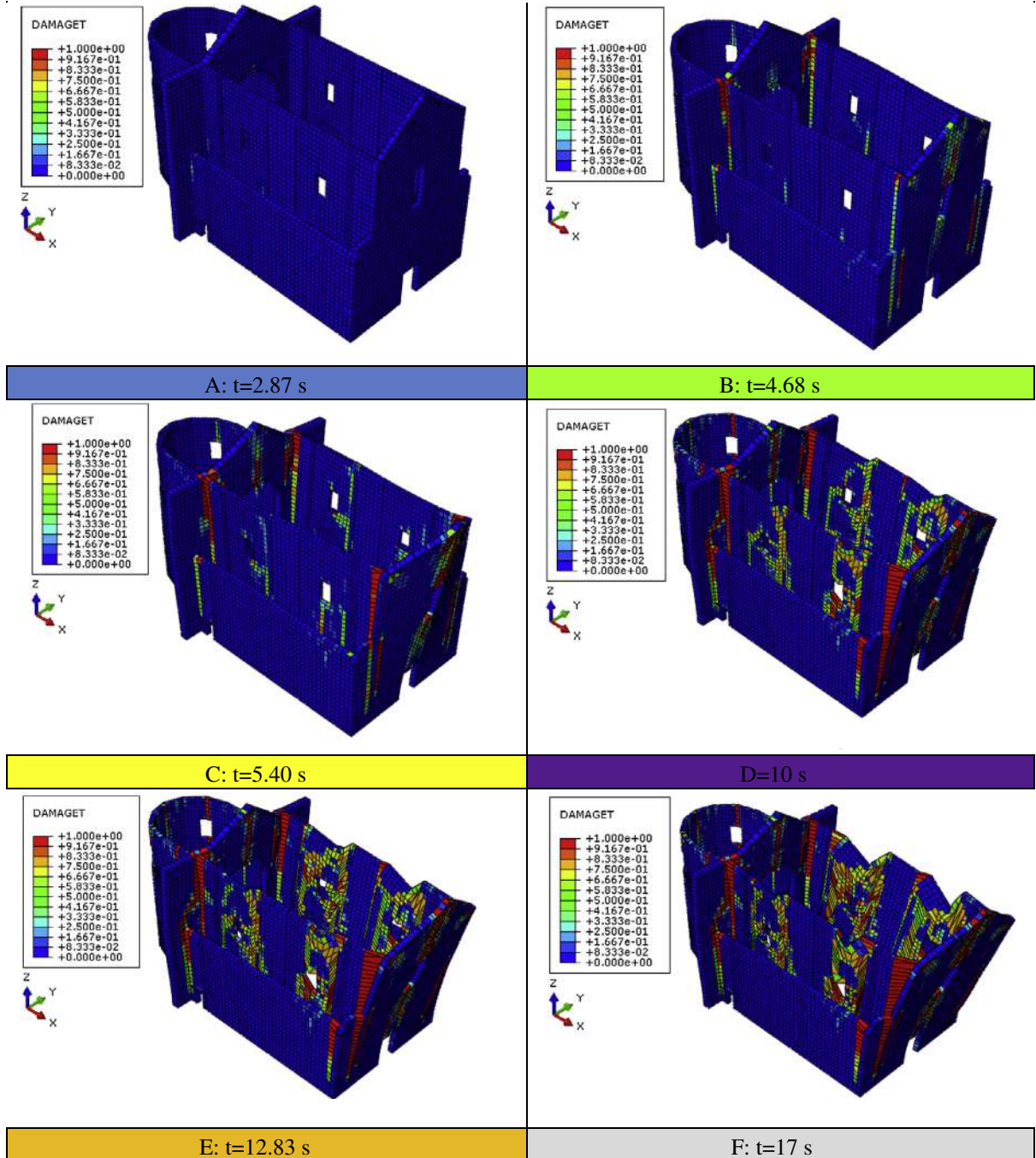


Fig. 11. Church 1. Seismic excitation in the longitudinal direction of the church. Deformed shape at different instants during the time-history with indication of damage (red, 1: full damage; blue, 0: no damage). (For interpretation of the references to color in this figure legend, the reader is referred to the web version of this article.)

utilized. However, it is commonly accepted in the literature the utilization of isotropic models (like concrete smeared crack approach available in both Ansys and Adina) after an adaptation of the parameters to fit an average behavior between vertical and horizontal compression. A suitable model should also take into account the ratio between the ultimate compression strength in biaxial stress states and in uniaxial conditions. Such a ratio, which exhibits some similarities between concrete and masonry, is reasonably set equal to 1.16.

In tension, the stress-strain response follows a linear-elastic relationship, until the peak stress σ_{t0} is reached. Then, microcracks start to propagate in the material, a phenomenon which is macroscopically represented by softening in the stress-strain relationship. Under axial compression, the response is linear up to the value of the yield stress σ_{co} . After the yield stress, the response is typically characterized by hardening, which anticipates compression crushing, represented by a softening branch beyond the peak stress σ_{cu} .

Damage variables in tension and compression are defined by means of the following standard relationships:

$$\begin{aligned}\sigma_t &= (1 - d_t)E_0(\varepsilon_t - \varepsilon_t^{pl}) \\ \sigma_c &= (1 - d_c)E_0(\varepsilon_c - \varepsilon_c^{pl})\end{aligned}\quad (1)$$

where σ_t (σ_c) is the mono-axial tensile (compressive) stress, E_0 is the initial elastic modulus, ε_t (ε_c) is the total strain in tension (compression), ε_t^{pl} (ε_c^{pl}) is the equivalent plastic strain in tension (compression). In the present study, damage is assumed

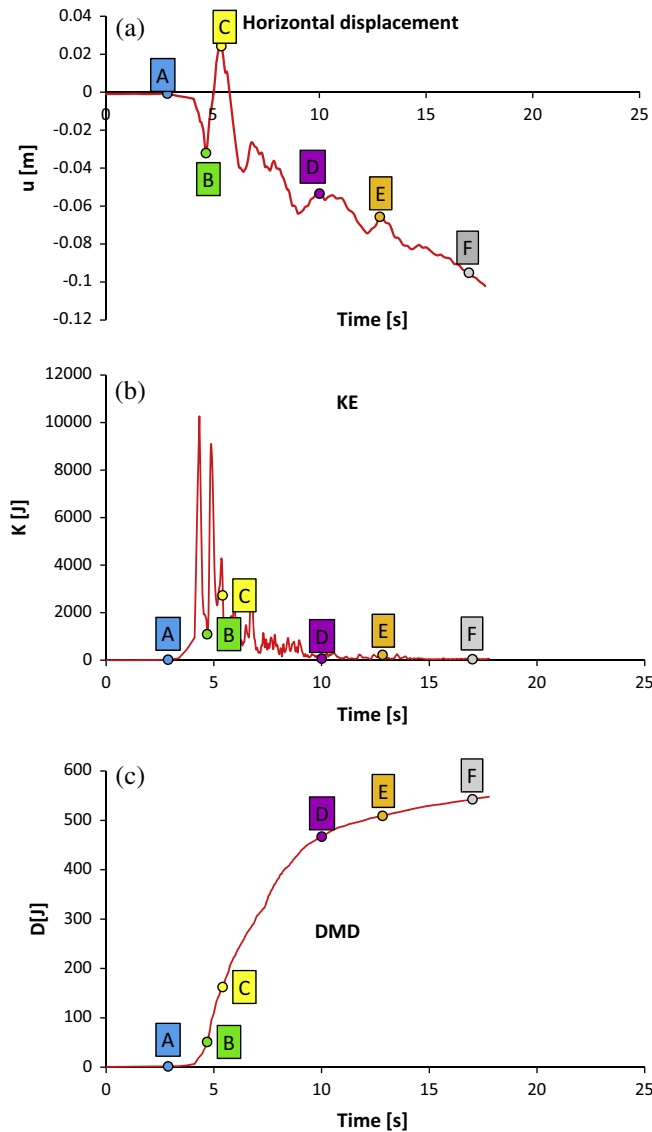


Fig. 12. Church 1. Seismic excitation in the transversal direction of the church. (a) Control point horizontal displacement time-history diagram. (b) Kinetic energy time-history diagram. (c) Energy dissipation in tension time-history diagram.

active in tension only, since the tensile strength of the material is very low, especially in comparison with the compressive one. When strain reaches a critical value, the material elastic modulus degrades in the unloading phase to $E < E_0$. In particular, within the simulations, a reduction equal to 5% of the elastic modulus with respect to the initial value is assumed for a plastic deformation equal to 0.003.

The issue of the mechanical properties to adopt for the constituent materials results particularly interesting. It is common opinion, indeed, that the major damages registered in historical buildings, such as towers, castles and churches, are a

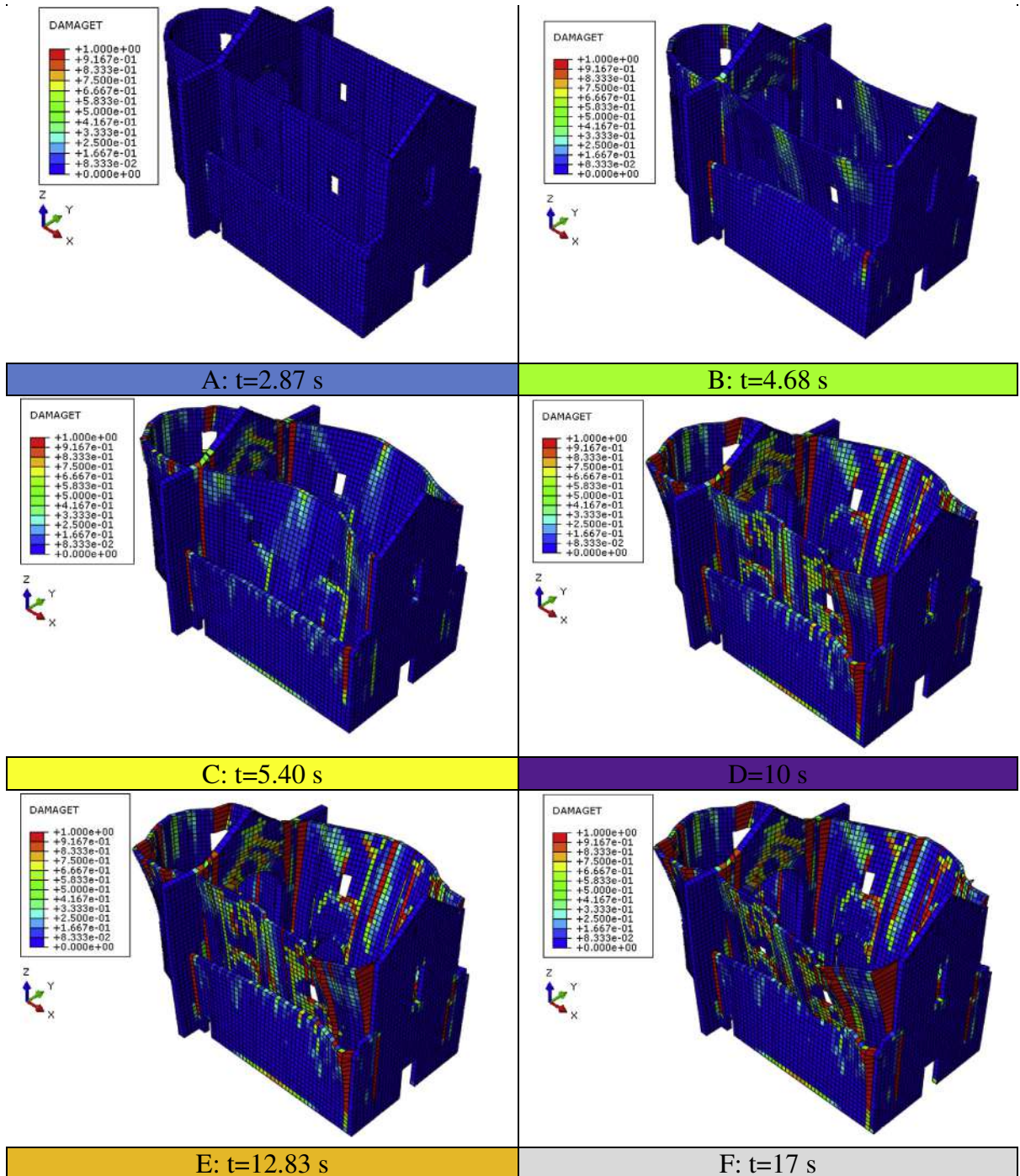


Fig. 13. Church 1. Seismic excitation in the transversal direction of the church. Deformed shape at different instants during the time-history with indication of damage (red, 1: full damage; blue, 0: no damage). (For interpretation of the references to color in this figure legend, the reader is referred to the web version of this article.)

consequence of very poor mechanical properties of joints, whereas clay bricks exhibit a quite high strength. Post-collapse surveys and photos taken after the main shocks, where intact stacks of bricks without mortar are visible, fully support this conclusion.

In absence of ad-hoc experimental campaigns performed on the case studies at hand, it is necessary to refer to what stated by Italian Code for existing masonry buildings. As a matter of fact, masonry is a material which exhibits distinct directional properties due to the mortar joints, acting as planes of weakness.

Considering the well-known limitation of use of both micro-modeling and homogenization at large scale, [45,46,47,48], isotropic macro-models are adopted for masonry. The reason for adopting an isotropic material stands in the impossibility to evaluate many parameters necessary for anisotropic materials in the inelastic range, in absence of ad-hoc experimental characterizations. Finally, it is worth noting that commercial codes rarely put at disposal to users anisotropic mechanical models suitable to describe masonry with regular brick pattern in the non-linear range.

According to Italian Code NTC 2008 [38], Chapter 8, and subsequent Explicative Notes [39], the mechanical properties assumed for masonry material depend on the so-called knowledge level LC, which is related to the so-called Confidence Factor FC. There are three LCs, labeled from 1 to 3, related to the knowledge level about the mechanical and geometrical properties of the structure. The knowledge level LC3 is the maximum, whereas LC1 is the minimum. For the cases at hand, a LC1 level is assumed in absence of specific in-situ test results.

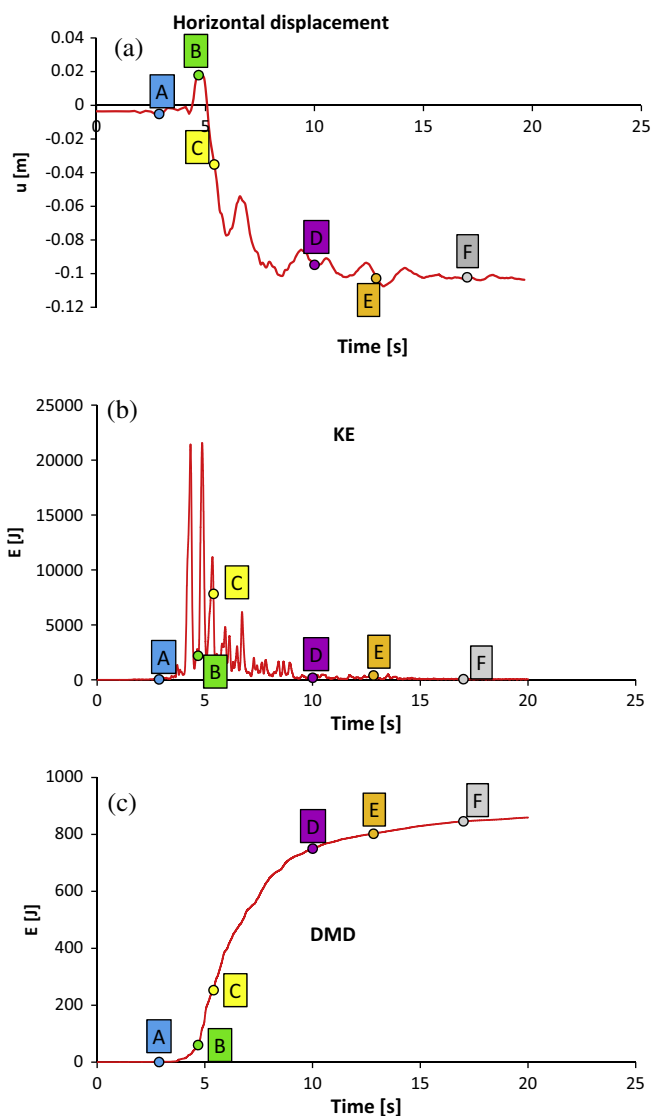


Fig. 14. Church 2. Seismic excitation in the longitudinal direction of the church. (a) Control point horizontal displacement time-history diagram. (b) Kinetic energy time-history diagram. (c) Energy dissipation in tension time-history diagram.

Confidence Factor FC summarizes the knowledge level regarding the structure and the foundation system, from a geometric and mechanical point of view. It can be determined defining different partial confidence factors F_{Ck} ($k = 1, 4$), on the basis of some numerical coefficients present in Italian Code (Table 4.1 Italian Guidelines). Due to the limited knowledge level achieved in this case, the highest confidence factor ($FC = 1.35$) was used.

After visual inspections, the values adopted for cohesion and masonry elastic moduli are taken in agreement with Table C8A.2.1 of the Explicative Notes [39], assuming a masonry typology constituted by clay bricks (a so-called Ferraresi bricks typology is present in all cases, with approximate dimensions equal to $300 \times 60 \times 100 \text{ mm}^3$) with very poor mechanical properties of the joint and quite regular courses.

Considering the lowest knowledge level LC (confidence factor $FC = 1.35$), Italian Code requires to select, in Table C8A.2.1, the lower bound values for strength and the average values between lower and upper bound for elastic moduli.

The application of the acceleration time-history occurs at the second step, where the structure is unrestrained using trailers, thus allowing it to move along the direction of the seismic action. As mentioned above, a real accelerogram recorded during the first seismic shake in Mirandola (20th May) is adopted. In particular, accelerations recorded between 30 and 50 s are used as input data, with the aim of cutting meaningfulness queues. The conventionally scaled accelerogram shown in Fig. 9 is finally adopted in order to take into consideration the average distance of the churches from the epicenter and make the computations comparable.

The numerical analyses are carried out by means of a dynamic approach with implicit integration in the time domain, using a time step equal to 0.005 s, which corresponds to the accelerogram registration time interval. The results of the

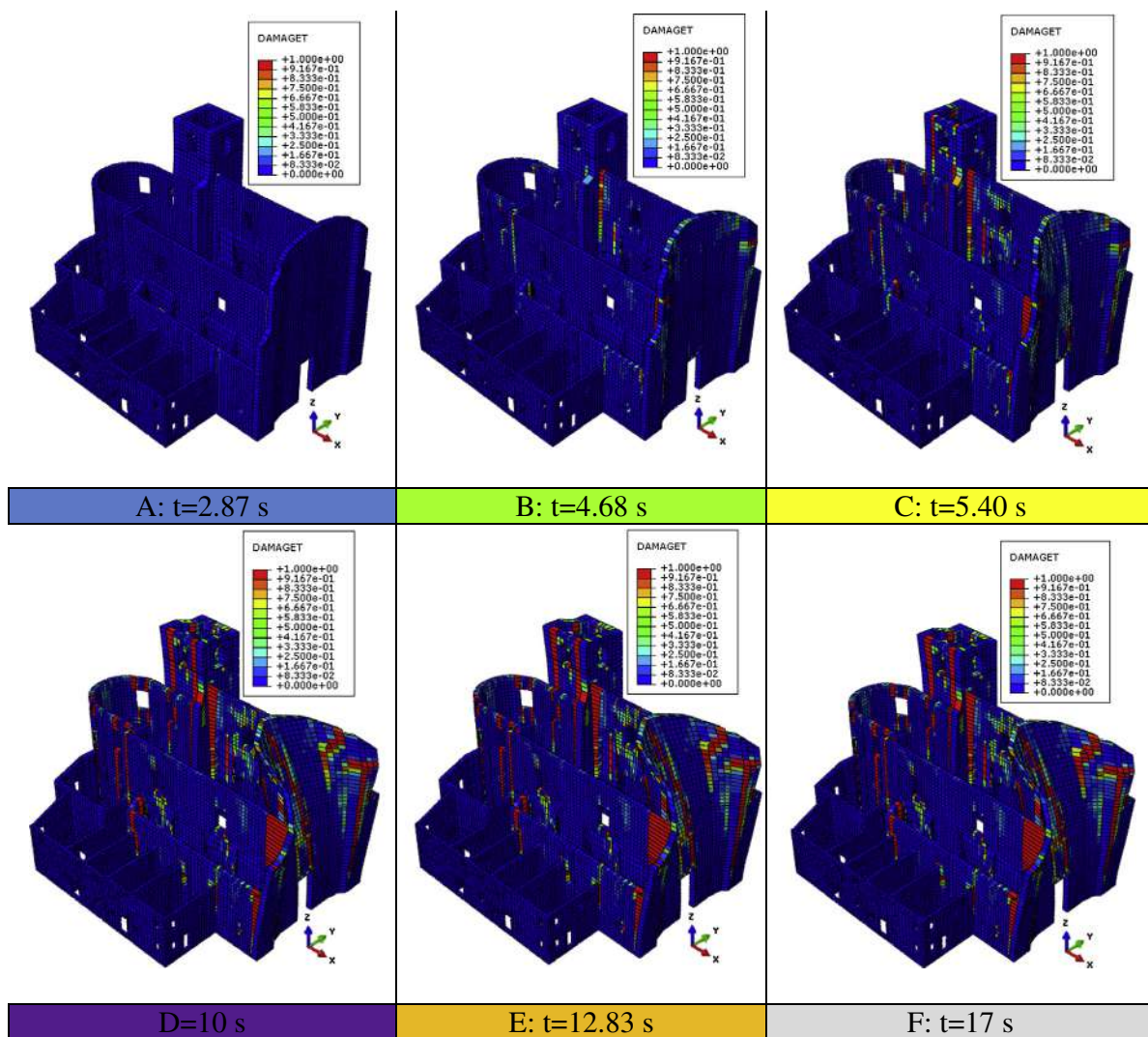


Fig. 15. Church 2. Seismic excitation in the longitudinal direction of the church. Deformed shape at different instants during the time-history with indication of damage (red, 1: full damage; blue, 0: no damage). (For interpretation of the references to color in this figure legend, the reader is referred to the web version of this article.)

analyses conducted in this study are reported in the following sections. The analyses were performed applying, separately, an accelerogram along the longitudinal and transversal directions of each church.

4. Results of the non-linear dynamic analyses

A concise synopsis of the huge amount of numerical results obtained from non-linear dynamic analyses is provided for each church. In particular, the following issues are discussed, also in comparison with the results provided by other approaches of analysis:

- (1) Activation or not of a failure mechanism at the end of the seismic excitation.
- (2) If a failure mechanism is active, displacement time-history of a control point. Such a diagram is useful to have an insight into the magnitude of the displacement and hence to estimate if the failure mechanism is active or partially active, i.e. if there are still additional resources available before collapse.
- (3) Contour plots of damage parameters (especially in tension, considering the low masonry strength) at successive instants. Damage evolution is also useful to clearly identify the critical zones of the structure and the most probable active failure mechanisms.

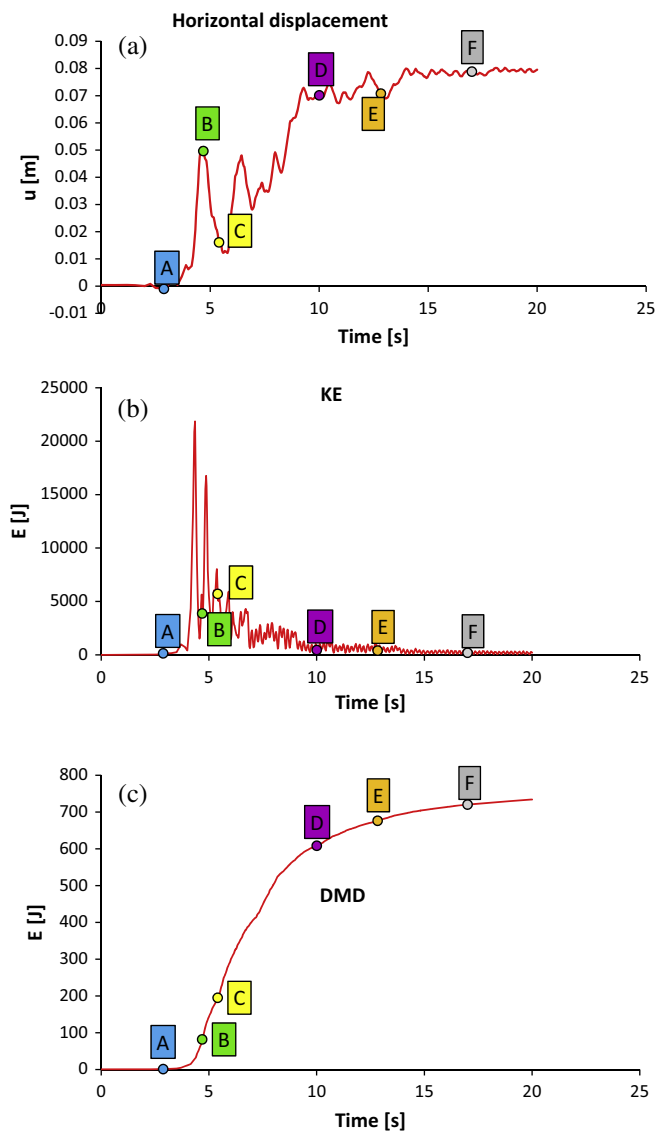


Fig. 16. Church 2. Seismic excitation in the transversal direction of the church. (a) Control point horizontal displacement time-history diagram. (b) Kinetic energy time-history diagram. (c) Energy dissipation in tension time-history diagram.

Some meaningful instants of the simulations are investigated in detail and are identified in the accelerogram of Fig. 9 with different letters and colors. The chosen instants are the following:

- Instant A (blue): first relevant ground motion acceleration peak;
- Instant B (green): negative acceleration peak;
- Instant C (yellow): positive acceleration peak;
- Instant D (purple): half time of the recorded ground motion;
- Instant E (orange): last relevant ground motion acceleration peak;
- Instant F (gray): practical end of the seismic excitation.

By means of the damage development sequence shown at the different instants, it is possible to have a deep insight into the formation of the failure mechanisms. In addition, it is possible to plot (1) the displacement time-history for a suitable control point, (2) the kinetic energy (KE) time-history and (3) the cumulative damage in tension (DMD) time-history.

From the displacement time-history of a selected node, it can be deduced if significant residual displacements are present at the end of the simulations. If there are considerable residual displacements, large inelastic deformation occurred. The damage contour plot at instant F, in conjunction with the magnitude of the residual displacement of the control point (it has to be ensured that the control point belongs to an active failure mechanism), allows determining (1) if there is a clear

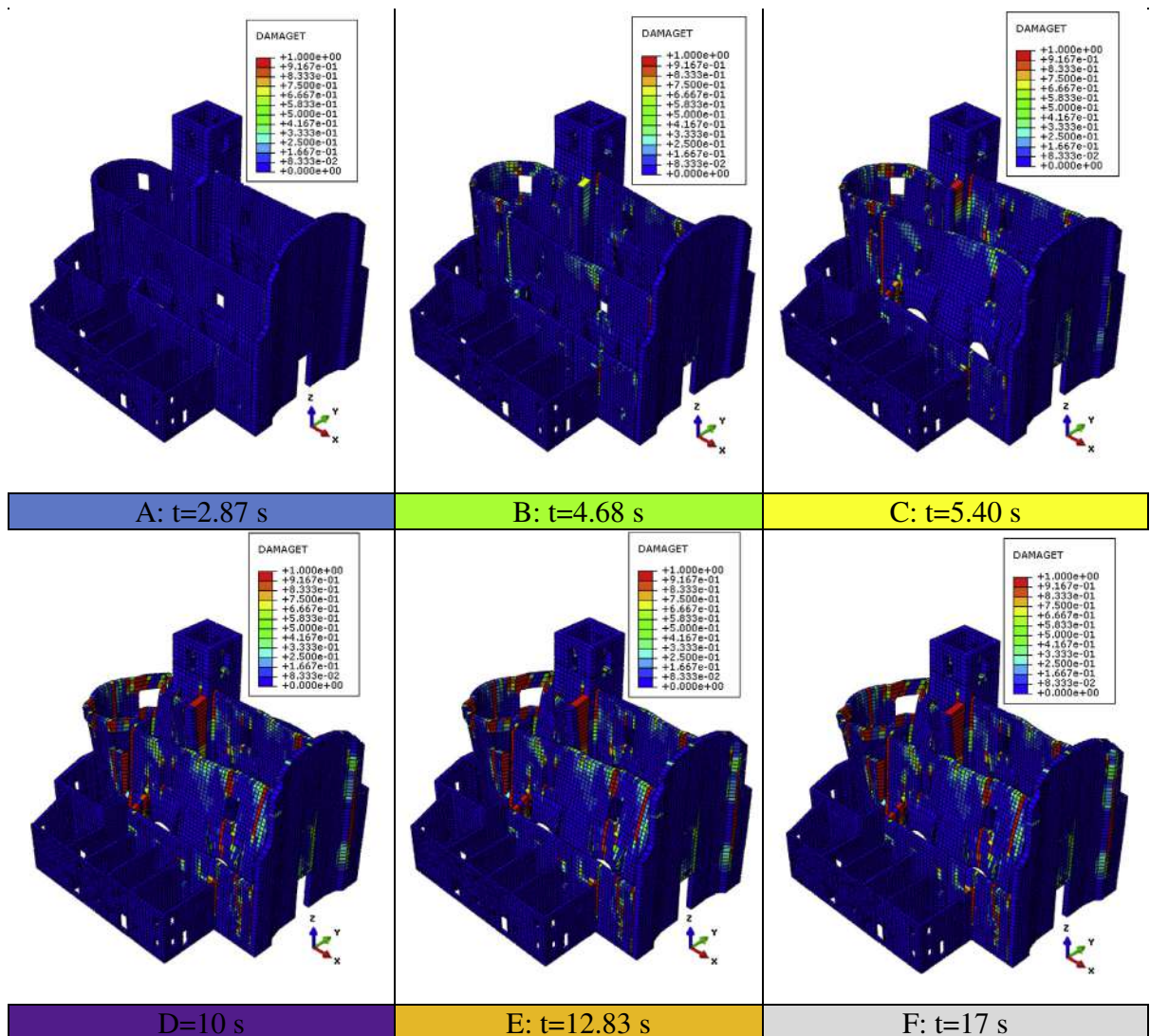


Fig. 17. Church 2. Seismic excitation in the transversal direction of the church. Deformed shape at different instants during the time-history with indication of damage (red, 1: full damage; blue, 0: no damage). (For interpretation of the references to color in this figure legend, the reader is referred to the web version of this article.)

activation of a partial collapse, (2) the typology of the mechanism and (3) if the magnitude of the displacement is still compatible with an un-collapsed state of the structure.

The evaluation of the kinetic energy (KE) time-history is useful to estimate if the structure is still moving or not at the end of the simulation. If a not negligible value of kinetic energy is found at the end of the seismic event and if the activation of a failure mechanism has not still occurred, then it is mandatory to proceed further with the analysis in order to determine if the residual kinetic energy may be responsible for additional damage and consequently for the activation of the structural collapse.

Similar information is given by the cumulative damage in tension (DMD) time-history. If damage cumulates, then cracks propagate. When damage asymptotically reaches a plateau value at the end of the simulations, it can be stated that a failure mechanism is active.

4.1. Church 1

The behavior of Church 1 under longitudinal and transversal seismic excitation is investigated by means of the model with damage previously described. The results of the analyses conducted are collected in Figs. 10–13. In particular, Figs. 10 and 11 refer to the application of the accelerogram in the longitudinal direction of the church, whereas Figs. 12 and 13 refer to the transversal direction, respectively.

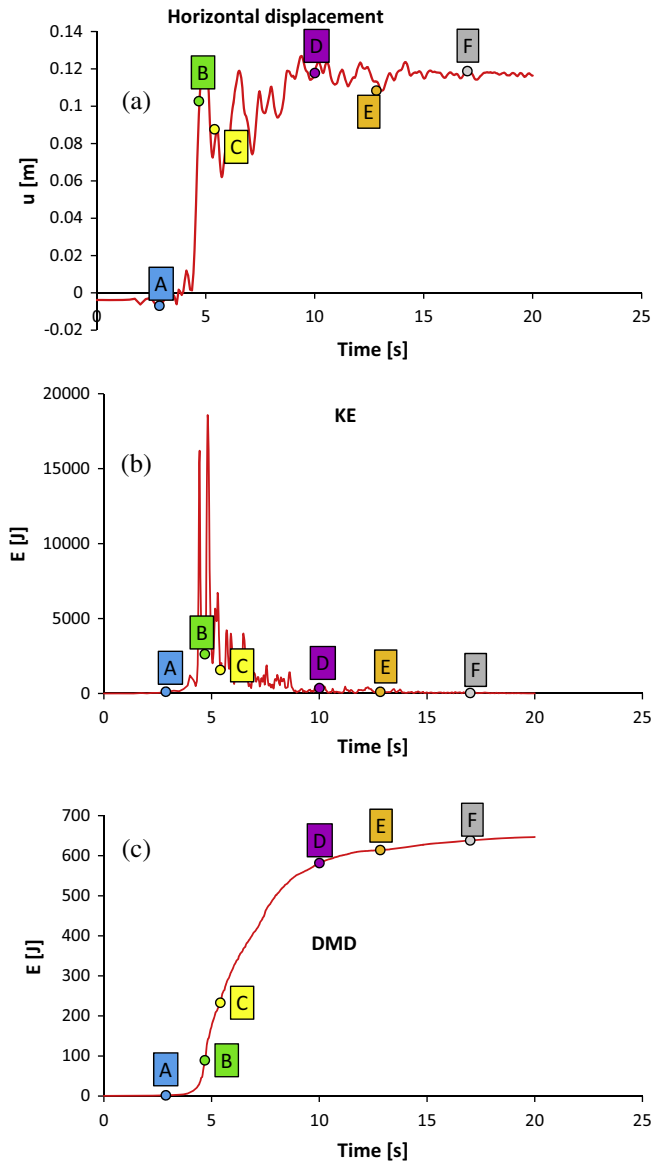


Fig. 18. Church 3. Seismic excitation in the longitudinal direction of the church. (a) Control point horizontal displacement time-history diagram. (b) Kinetic energy time-history diagram. (c) Energy dissipation in tension time-history diagram.

Deformed shapes of the structure at the practical end of the simulations (17 s) for longitudinal and transversal seismic action are depicted in Figs. 11 and 13, respectively. In the same figures, the contour plots of tension damage parameter are also represented; red color is associated to full (1) damage and blue color to zero (0) damage. As can be noted, when the seismic excitation is applied along the longitudinal direction of the church, the active failure mechanism is the overturning of the façade, with a clear detachment from perpendicular walls. The activation of such a collapse mechanism is confirmed by the diagrams of Fig. 10 (i.e. displacement, KE and DMD time-history). The residual displacement of the control point (top edge of the façade tympanum) is around 30 cm. KE is negligible at the end of the simulations, which means that the structure remains in its deformed configuration, i.e. the failure mechanism is active but does not proceed further. Accordingly, DMD reaches an asymptotic value.

When the seismic action is applied in the transversal direction of the church, the control point is located in the middle of the top edge of one of the perimeter walls. As can be noted from the deformed shapes and from damage contour plots at the different instants depicted in Fig. 13, the active failure mechanism is characterized by the out-of-plane failure of the nave walls. In the framework of the dynamic analyses, both of them may be considered as collapsed, exhibiting a similar overturning behavior.

It is interesting to notice that also the triumphal arch and the apse show active crack patterns. The residual displacements of the apse are lower than those of the nave, but still meaningful. The strength of the triumphal arch, being loaded in-plane, results far higher than that of perimeter walls.

Horizontal displacement, KE and DMD diagrams reported in Fig. 12 show common features with those found for earthquake acting along the longitudinal direction of the church, i.e. residual displacement of the control point not consistent with the equilibrium of the structure under small displacements, negligible kinetic energy at the end of the simulation and cumulative damage reaching an asymptote. From a comparative analysis of the results, it can be therefore stated that the out-of-plane failure of perimeter longitudinal walls occurred.

4.2. Church 2

The results of the dynamic analyses carried out on Church 2 are collected from Figs. 14–17. As for the previous case, Figs. 14 and 15 refer to the longitudinal direction of application of the seismic excitation, whereas Figs. 16 and 17 refer to the transversal one.

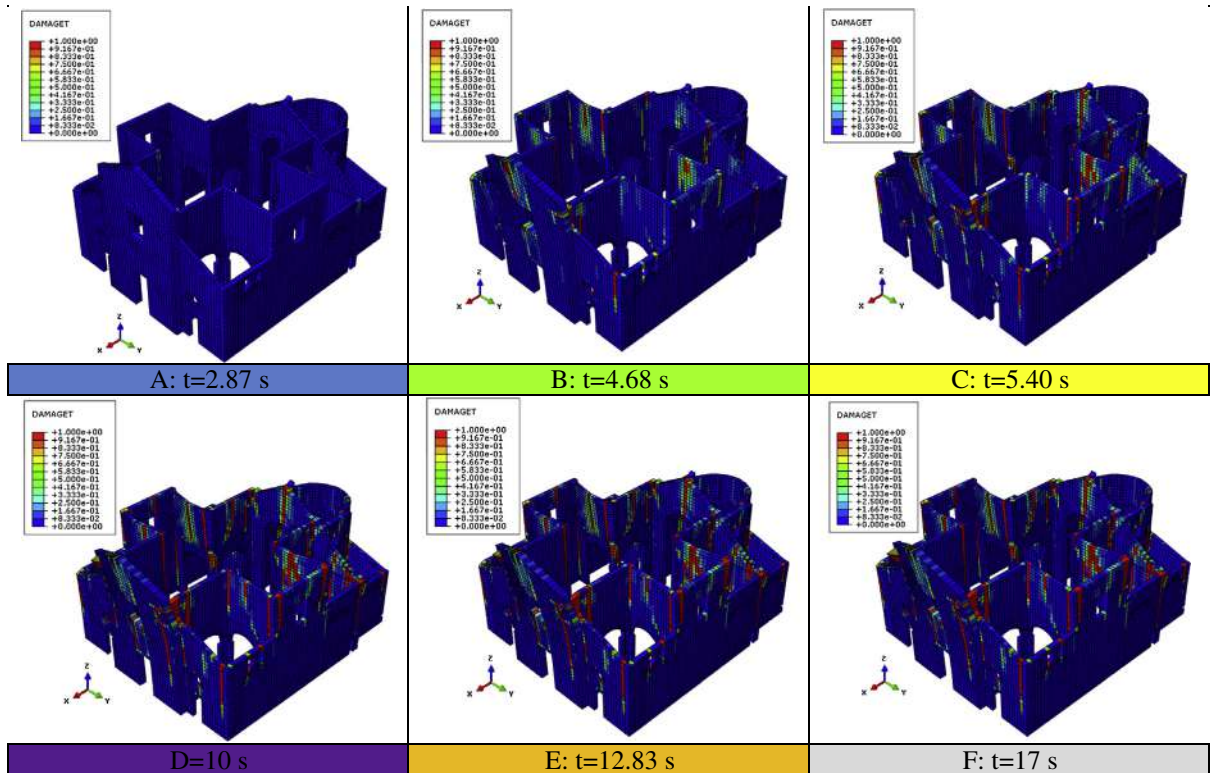


Fig. 19. Church 3. Seismic excitation in the longitudinal direction of the church. Deformed shape at different instants during the time-history with indication of damage (red, 1: full damage; blue, 0: no damage). (For interpretation of the references to color in this figure legend, the reader is referred to the web version of this article.)

The evolution of damage at different instants is represented in Fig. 15 (longitudinal direction) and Fig. 17 (transversal direction). Similarly to the previous case, for the longitudinal direction the active macro-block is represented by the upper portion of the façade, whereas for the transversal one it is represented by the lateral walls, with quite relevant concentration of damage in the apse and the bell tower too.

The façade collapse is characterized by visible vertical cracks between façade and nave walls, probably promoted by its curved shape and the stiffening pillars. The formation of inclined yield lines results into residual displacements not exceeding 10 cm, see Fig. 14, which is a value however compatible with the activation of a failure mechanism. The behavior under transversal seismic action is complicated by the bell tower, embedded into the church, which exhibits visible vertical cracks in the model, splitting the structure into two portions. Finally, the apse overturns laterally around a hinge located near the base.

4.3. Church 3

A synopsis of the results of the dynamic analyses performed on Church 3 is reported from Figs. 18–21. In particular, the longitudinal behavior is summarized in Fig. 18 (displacement, KE and DMD time-history) and in Fig. 19 (damage evolution and amplified deformed shapes at different instants). The same diagrams/figures are replicated for the transversal response in Fig. 20 and 21.

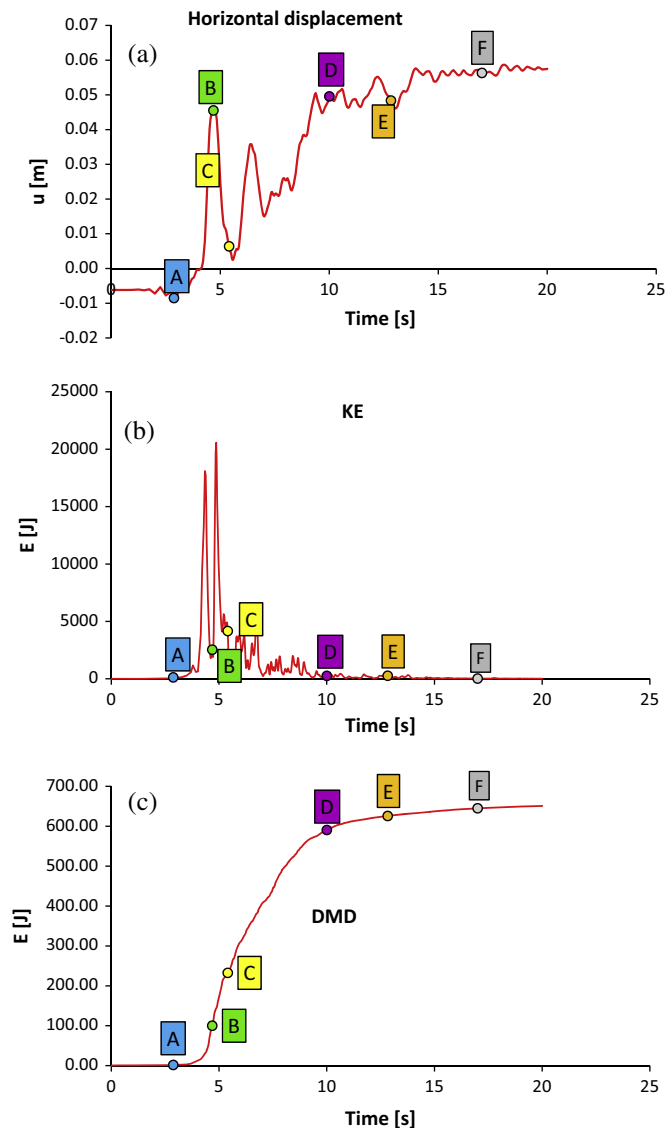


Fig. 20. Church 3. Seismic excitation in the transversal direction of the church. (a) Control point horizontal displacement time-history diagram. (b) Kinetic energy time-history diagram. (c) Energy dissipation in tension time-history diagram.

From the dynamic analyses, it can be argued that the active failure mechanism is the façade overturning when the seismic action is applied in the longitudinal direction of the church. However, the in-plan complexity of the structure, with the presence of squat chapels slightly asymmetrical, results into a visible torsional movement of the façade on the horizontal yield line forming near the base, as well as into damage diffused on all the walls of the transept and on the triumphal arch.

The application of the same accelerogram along the transversal direction of the church results into the simple overturning of one of the lateral walls, with a clear formation of a base cylindrical hinge. The wall has a complex geometry and is interconnected with several perpendicular structural elements (e.g. façade, transept, apse). Despite the very low masonry strength, in this case geometry constraints secure a not negligible additional strength, precluding the overturning of the wall by the total formation of the mechanism, easily predictable with simplified approaches. As a matter of fact, the residual displacement of the control node (placed on the top edge) at the end of the simulation, see Fig. 20, appears to stand on the border-line to consider the partial collapse totally activated.

4.4. Church 4

The results of the dynamic analyses carried out on Church 4 are depicted from Figs. 22–26. In particular, the longitudinal behavior is summarized from Figs. 22–24, whereas the transversal response in Figs. 25 and 26.

When the seismic action is applied in the longitudinal direction of the church, an overturning of the façade occurs in the numerical simulations, with formation of a straight yield line at the base of the structure. A residual displacement of 12 cm is found at the top of the tympanum (control point), fully consistent with the failure of the structure. It can be noted, however, that one wall of a lateral chapel fails before the façade, Fig. 24, with divergence of the horizontal displacement, see Fig. 22a. Divergence is confirmed by the kinetic energy plot, Fig. 22b, where a sudden increase is visible near the end of the simulation.

Similarly to the previous cases, the behavior under transversal seismic action is characterized by the out-of-plane damage of both the walls belonging to the nave, see Fig. 26. However, the residual displacement of the control node is about 6 cm, meaning that additional resources are still present before the activation of a failure mechanism. As a matter of fact, the lateral walls of the nave are regularly interconnected with perpendicular walls and such a geometric condition justifies both the relatively small displacements found at the end of the simulation and the additional strength resources still to activate.

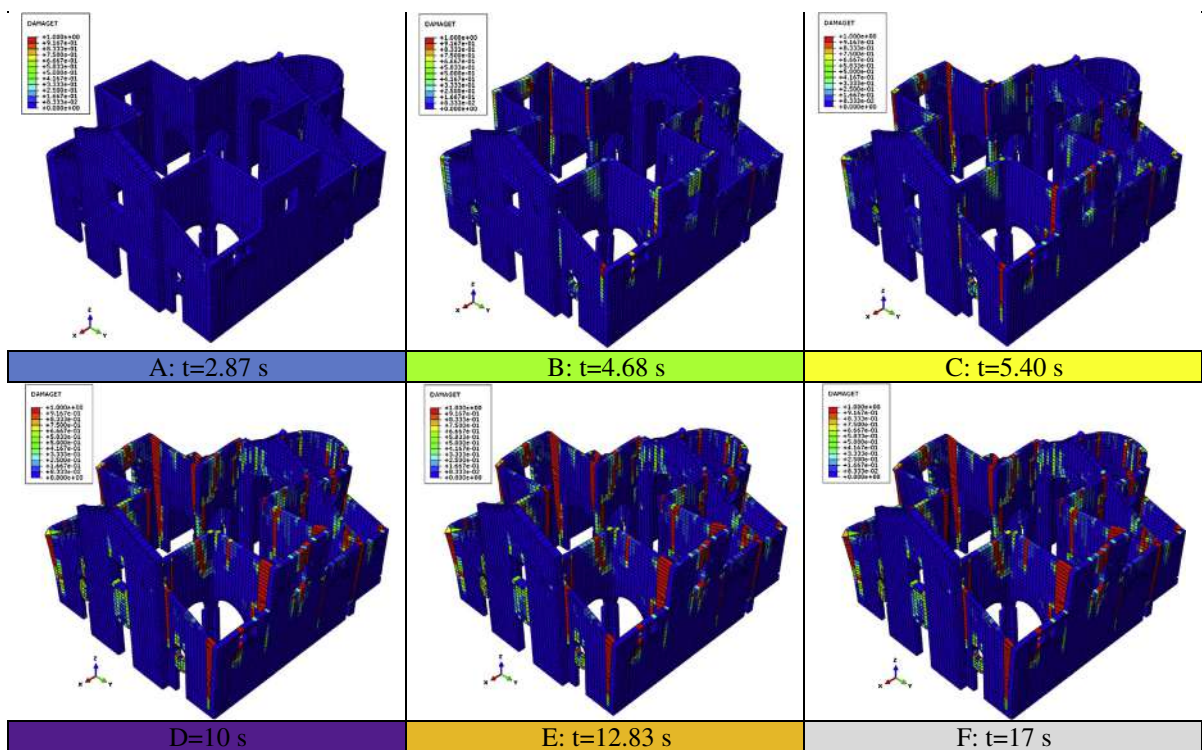


Fig. 21. Church 3. Seismic excitation in the transversal direction of the church. Deformed shape at different instants during the time-history with indication of damage (red, 1: full damage; blue, 0: no damage). (For interpretation of the references to color in this figure legend, the reader is referred to the web version of this article.)

4.5. Church 5

The results of the dynamic analyses performed on Church 5 are depicted from Figs. 27–30. The outcomes obtained under earthquake acting in the longitudinal direction of the church are reported in Figs. 27 and 28, whereas the response in the transversal direction is provided in Figs. 29 and 30.

Due to the simplicity of the geometry, the behavior of the church subjected to dynamic excitation is fully in agreement with simplified static procedures (the reader is referred to [11] for a detailed discussion of the results).

In particular, for the longitudinal direction, an overturning of the façade occurs, with a clear detachment from perpendicular walls and the formation of a straight yield line at the base of the structure. Residual displacements of 12 cm at the top of the wall (control point) are again consistent with failure due to overturning of the entire façade. It is interesting to notice that also the apse and the presbytery exhibit extensive damage in the upper part, which recalls the activation of the overturning of the upper portion around a horizontal hinge.

The behavior under transversal seismic action, as a consequence of the fact that nave walls are long and interconnected perpendicularly only with the triumphal arch and the façade, is characterized by the activation of an out-of-plane mechanism, see Fig. 30, with inclined yield lines spreading from the upper part of the vertical supports. The residual displacement of the control node is about 7 cm, meaning that additional resources are still present before the collapse. Kinetic energy and energy dissipation associated with damage confirm that there are no macro-blocks with active velocity components at the end of the simulations in both the longitudinal and transversal directions.

4.6. Church 6

The results of the dynamic analyses carried out on Church 6 are summarized in Figs. 31 and 32 for the longitudinal direction and in Figs. 33 and 34 for the transversal one.

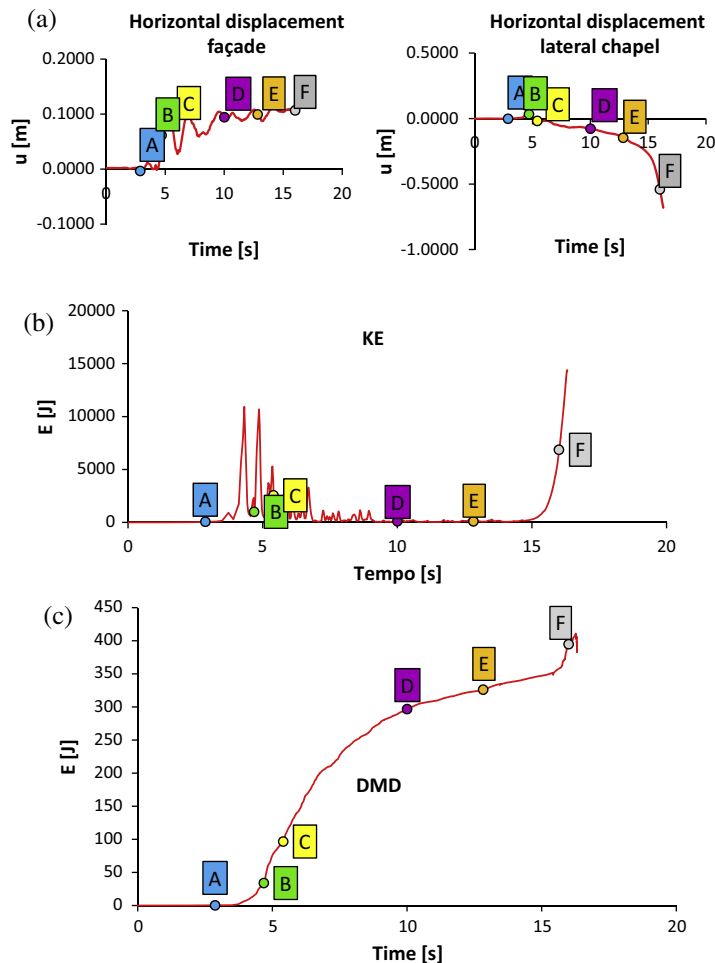


Fig. 22. Church 4. Seismic excitation in the longitudinal direction of the church. (a) Control point horizontal displacement time-history diagram. (b) Kinetic energy time-history diagram. (c) Energy dissipation in tension time-history diagram.

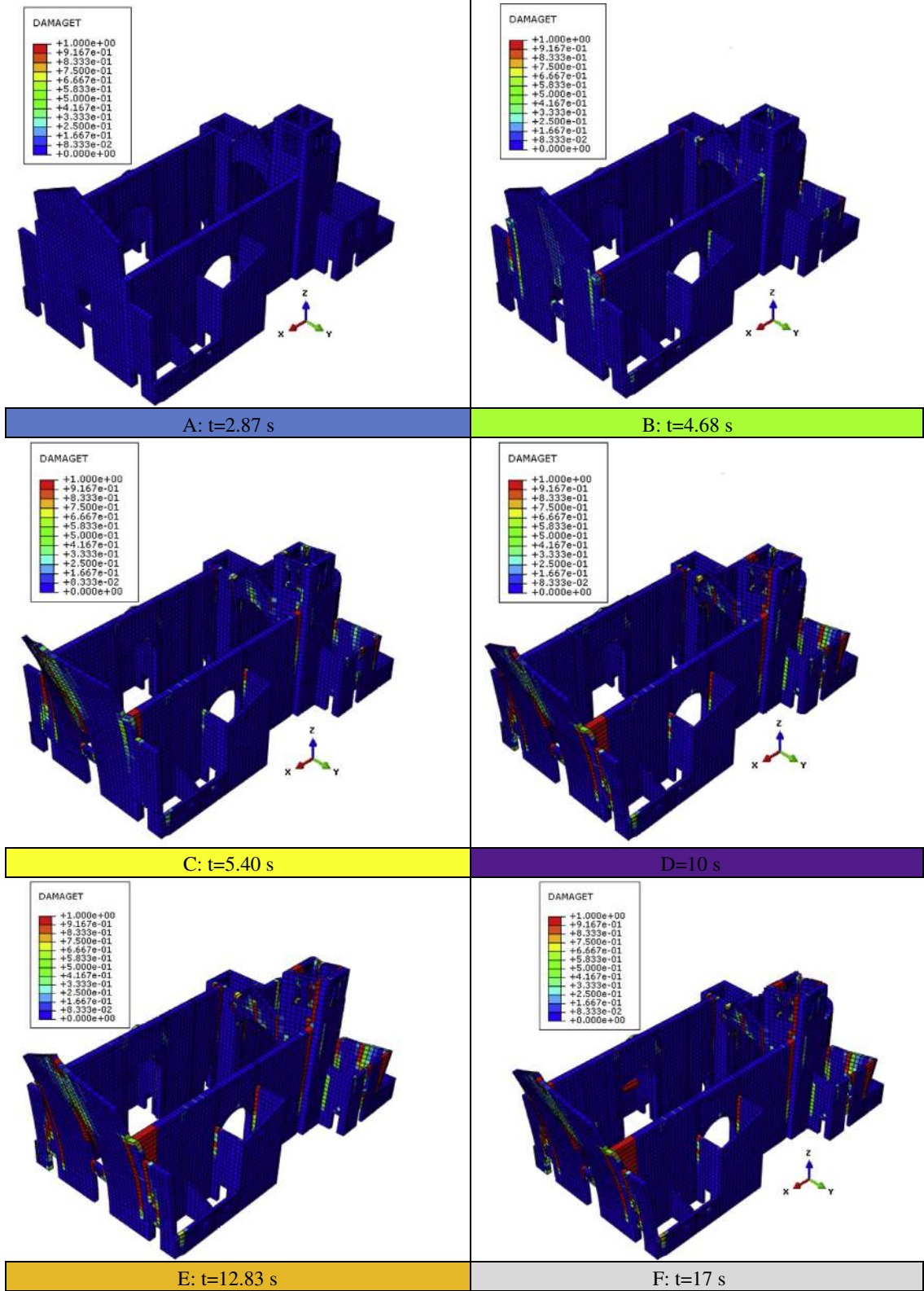


Fig. 23. Church 4. Seismic excitation in the longitudinal direction of the church. Deformed shape at different instants during the time-history with indication of damage (red, 1: full damage; blue, 0: no damage). (For interpretation of the references to color in this figure legend, the reader is referred to the web version of this article.)

As can be noted, the accelerogram applied along the longitudinal direction of the church causes the failure of the façade, with a significant crack pattern in the apse, as partially observed during the seismic sequence occurred in 2012. The residual maximum displacement of the control node (at the level of the tympanum) is about 14 cm, see Fig. 31, meaning that the failure mechanism is almost totally active and that the hypothesis of small displacements results questionable.

The behavior under earthquake acting along the transversal direction of the church shows, in partial disagreement with predictions provided by static analyses (limit and pushover analyses, the reader is referred to [11] for a detailed discussion of the results), a damage concentration in the triumphal arch, see Fig. 34, with the formation of two almost vertical yield lines

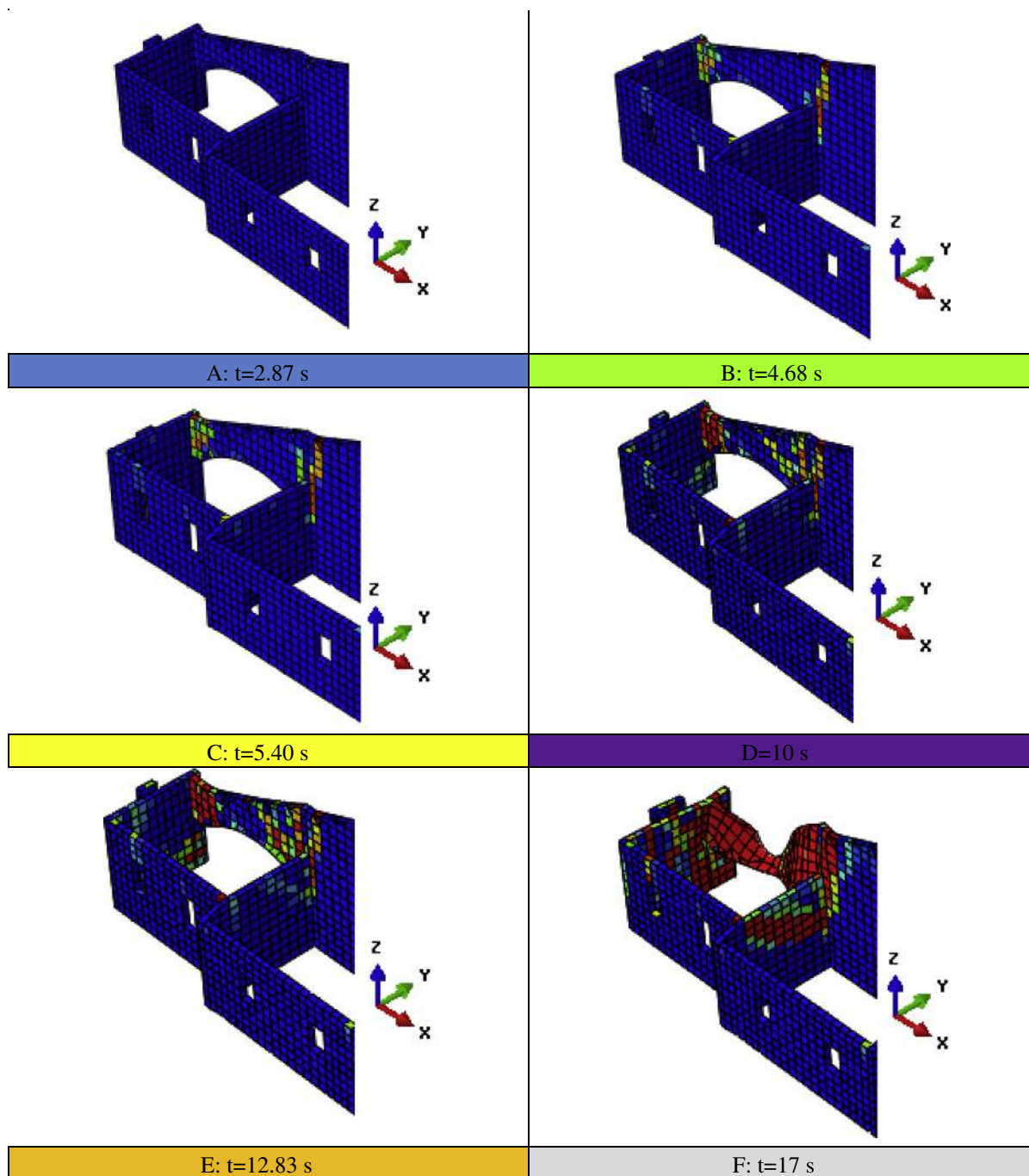


Fig. 24. Church 4. Seismic excitation in the longitudinal direction of the church. Detail of deformed shape at different instants during the time-history with indication of damage (red, 1: full damage; blue, 0: no damage). (For interpretation of the references to color in this figure legend, the reader is referred to the web version of this article.)

spreading from the upper part of both piers to the roof. The residual displacement of the control node (top of the roof) is about 30 cm, see Fig. 33, which is a value considered largely outside the deformation capacity of the structure to guarantee equilibrium.

The plots of the kinetic energy and of the energy dissipation associated with damage, see Fig. 33b and c respectively, show a strong reduction of the velocities at the end of the simulations (i.e. failure mechanisms are no longer active) and an almost horizontal asymptote of the cumulative damage (i.e. the formed crack pattern is stable and is not proceeding further).

4.7. Church 7

The results of the dynamic analyses performed in the longitudinal direction of Church 7, see Figs. 35 and 36, show the formation of a failure mechanism of the façade, due to the overturning around a cylindrical hinge placed near the base. Visible damage is also observed on the apse and along the lateral walls of the central nave. The overturning of the façade results slightly asymmetric, probably due to the asymmetries of both the lateral chapels and the contiguous buildings attached in correspondence of the apse. The failure mechanism is in partial agreement with the results provided by limit analysis, see [11], where the inelastic deformation is almost totally concentrated on both the façade and the upper part of the apse, whereas the results provided by non-linear static analyses exhibit convincing similarities with present

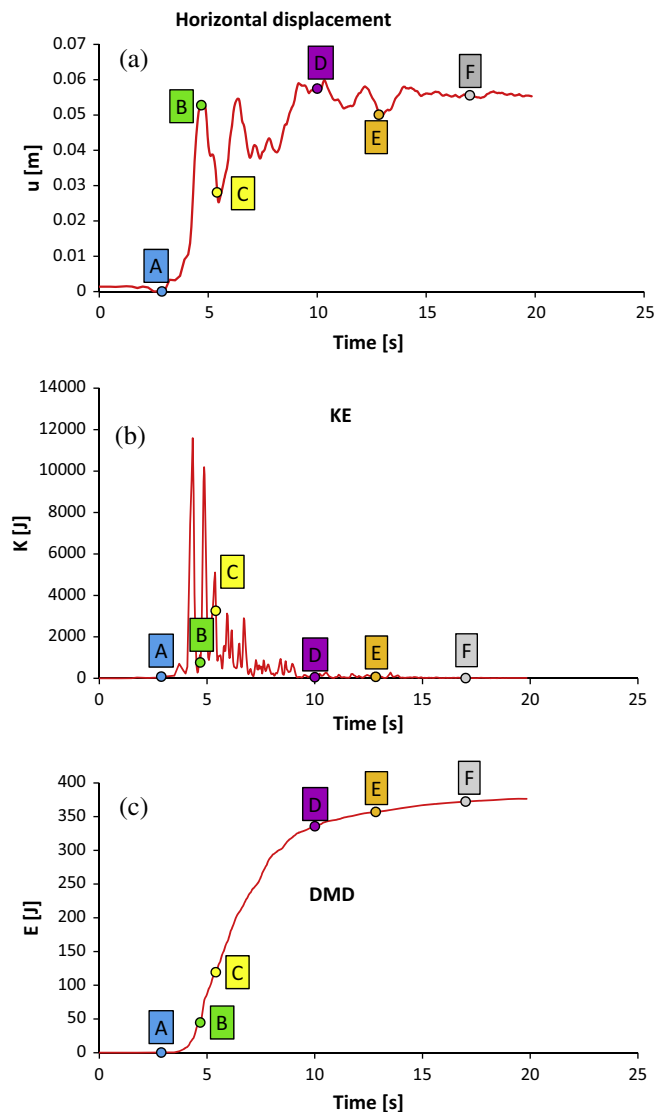


Fig. 25. Church 4. Seismic excitation in the transversal direction of the church. (a) Control point horizontal displacement time-history diagram. (b) Kinetic energy time-history diagram. (c) Energy dissipation in tension time-history diagram.

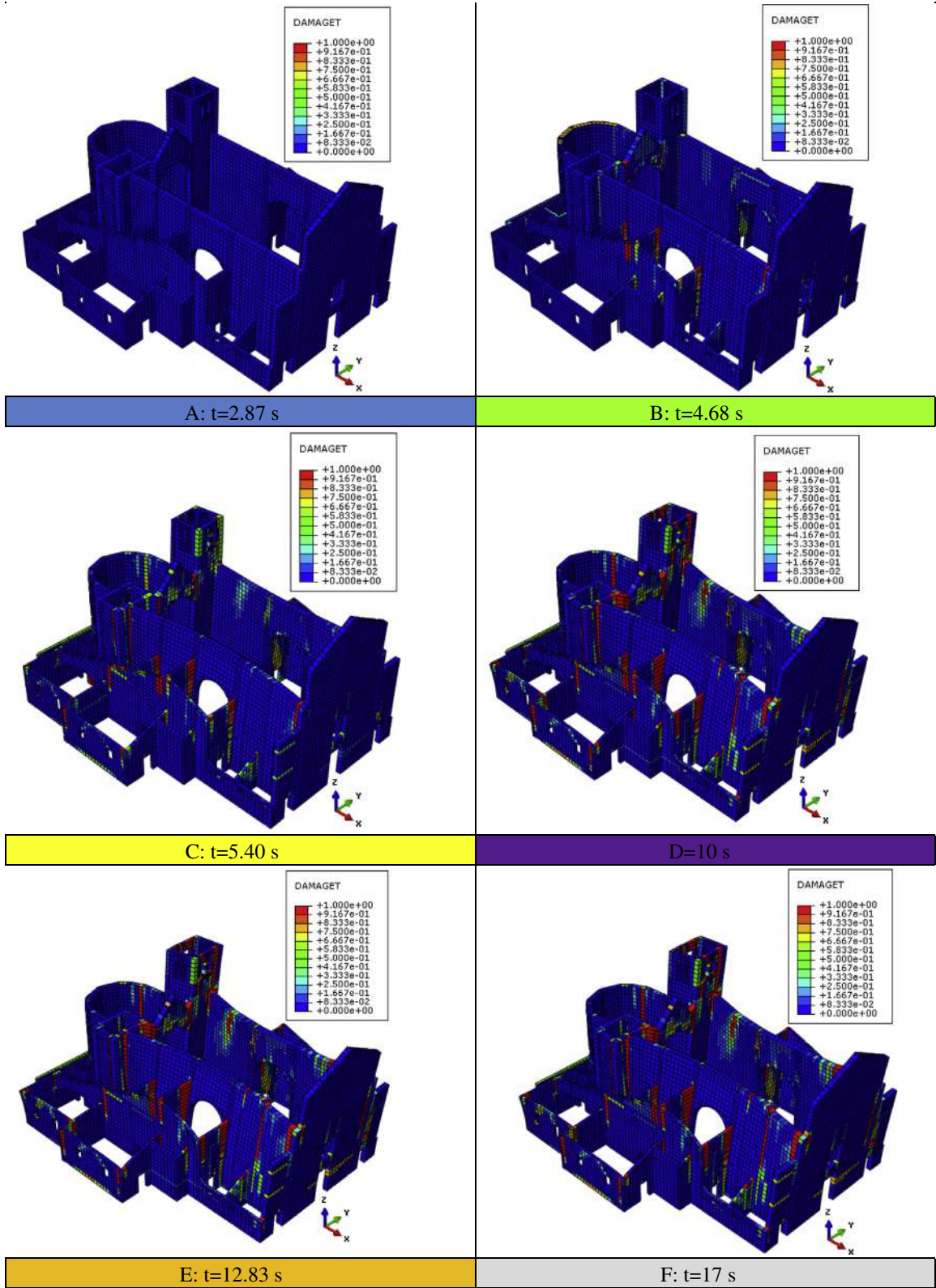


Fig. 26. Church 4. Seismic excitation in the transversal direction of the church. Deformed shape at different instants during the time-history with indication of damage (red, 1: full damage; blue, 0: no damage). (For interpretation of the references to color in this figure legend, the reader is referred to the web version of this article.)

non-linear dynamic simulations. The residual displacement registered at the top of the tympanum is about 15 cm, which is a value very similar to that found after the seismic event [11], again confirming that the failure mechanism is almost totally developed.

The results obtained when the seismic action is applied in the transversal direction of the church are summarized in Figs. 37 and 38. Again, the failure mechanism is in good agreement with both limit analysis and non-linear static approach [11], with the activation of a quite global mechanism involving both the lateral walls and the stiffening triumphal arches. The residual displacement is about 13 cm, a value that can be reasonably considered over the collapse state.

5. Comparison with other approaches of analysis

Some general conclusions can be drawn from the dynamic analyses conducted on the seven masonry churches at hand. The present study, indeed, should be considered in the framework of a wide sensitivity investigation, the results of which may be used for practical purposes in other specific cases and to methodologically study different examples. In particular, it can be stated that the different responses exhibited by different churches, under the same accelerogram and for the same material model, strictly depend on the global geometry of each structure, with particular regard to the in-plan irregularity.

In [10] and [11] the following numerical investigations have been carried out on the same case studies: (1) standard eigen-frequency analyses associated with response spectrum analyses; (2) pushover analyses using elastic-perfectly plastic

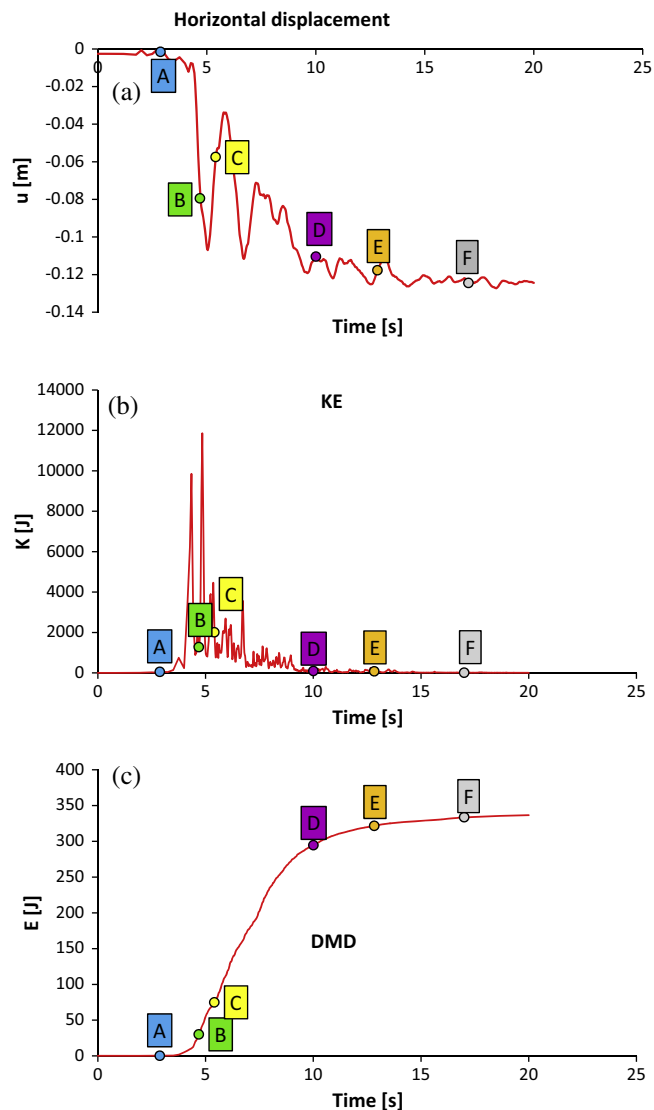


Fig. 27. Church 5. Seismic excitation in the longitudinal direction of the church. (a) Control point horizontal displacement time-history diagram. (b) Kinetic energy time-history diagram. (c) Energy dissipation in tension time-history diagram.

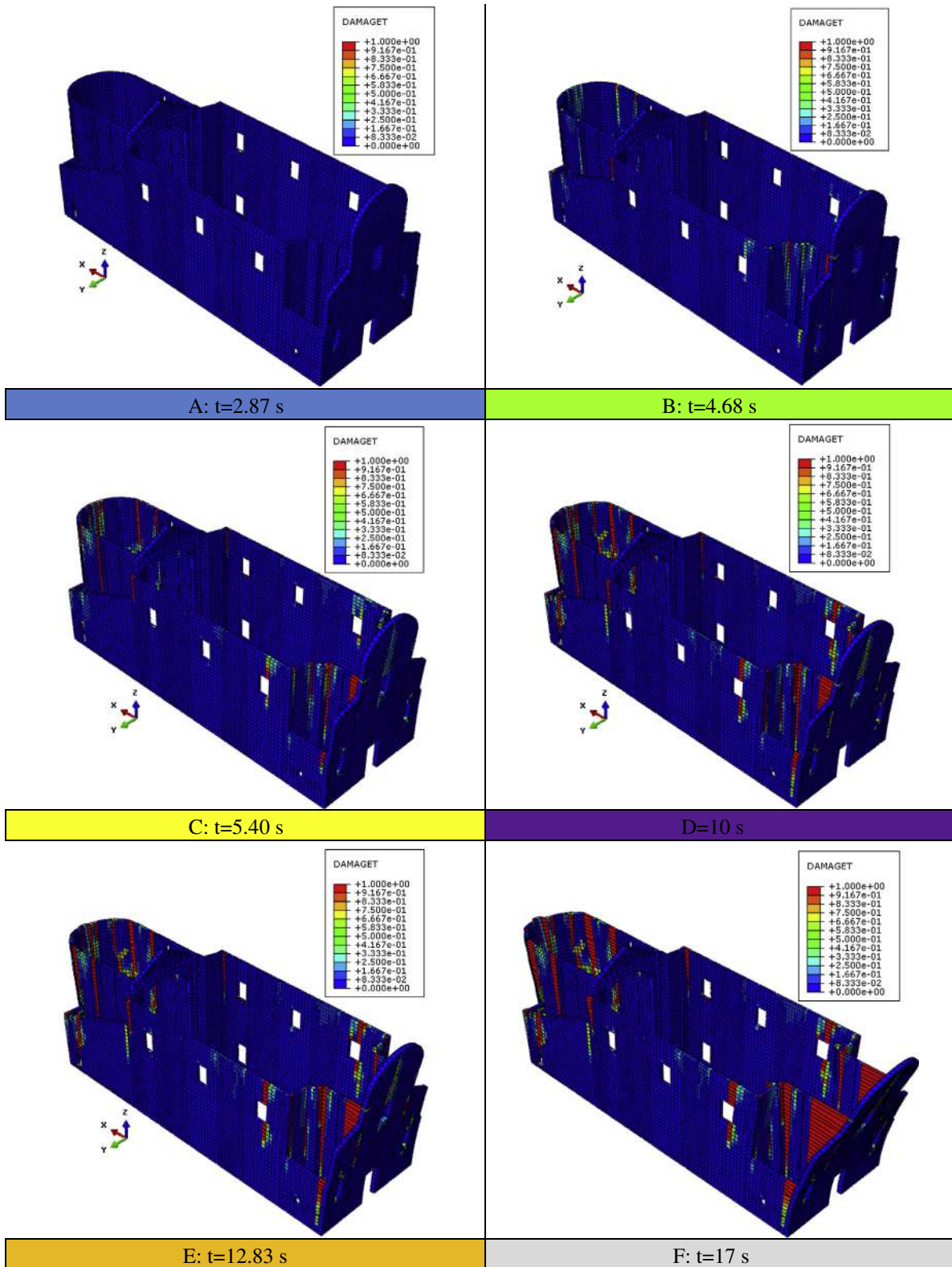


Fig. 28. Church 5. Seismic excitation in the longitudinal direction of the church. Deformed shape at different instants during the time-history with indication of damage (red, 1: full damage; blue, 0: no damage). (For interpretation of the references to color in this figure legend, the reader is referred to the web version of this article.)

materials with a Mohr–Coulomb failure criterion; (3) FE limit analyses (i.e. without pre-assigned failure mechanisms); (4) kinematic limit analyses as per prescription of Italian Code [28], i.e. where the failure mechanism is selected from 28 different pre-assigned collapse mechanisms.

In common seismic design a practitioner can adopt strategies (1) and (4), i.e. perform standard linear elastic response spectrum computations and evaluate the lowest acceleration associated with the activation of one of the 28 pre-assigned failure mechanisms, in agreement with the kinematic theorem of limit analysis applied to a material unable to withstand tensile stresses.

When dealing with pushover analyses according to strategy (2), it is worth mentioning that the utilization of an elastic-perfectly plastic material – which is questionable for masonry – comes from the effort by the authors to put at disposal to common designers a model directly manageable for users without a strong background on 3D FEs with brittle materials. On the other hand, it is stressed that Italian Guidelines on the Built Heritage [28] include the utilization of material models without softening during pushover analyses with 2D/3D models; in fact it is known that a global pushover curve with drop of the load bearing capacity is hardly reproducible for complex geometries and materials with very low tensile strength and good compression resistance.

Standard eigen-frequency analyses allow identifying – among other results and in the framework of linear elasticity – the vibration modes characterized by a high participating mass as well as the corresponding periods to compare with accelerations provided by either code response spectra or by accelerograms used in non-linear dynamic analyses. Albeit

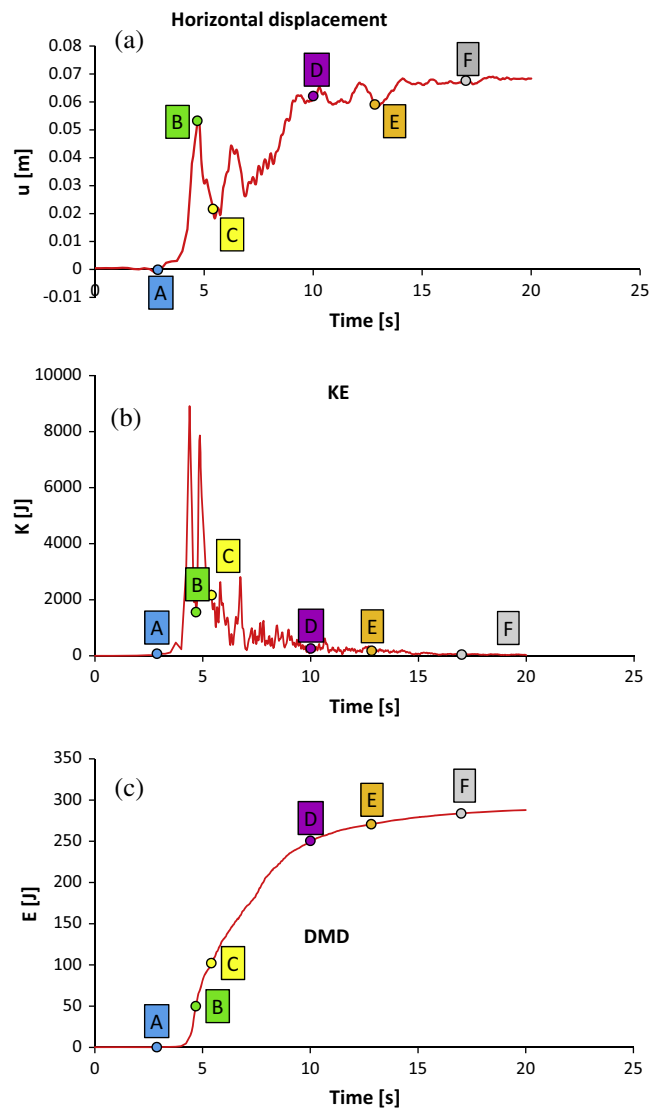


Fig. 29. Church 5. Seismic excitation in the transversal direction of the church. (a) Control point horizontal displacement time-history diagram. (b) Kinetic energy time-history diagram. (c) Energy dissipation in tension time-history diagram.

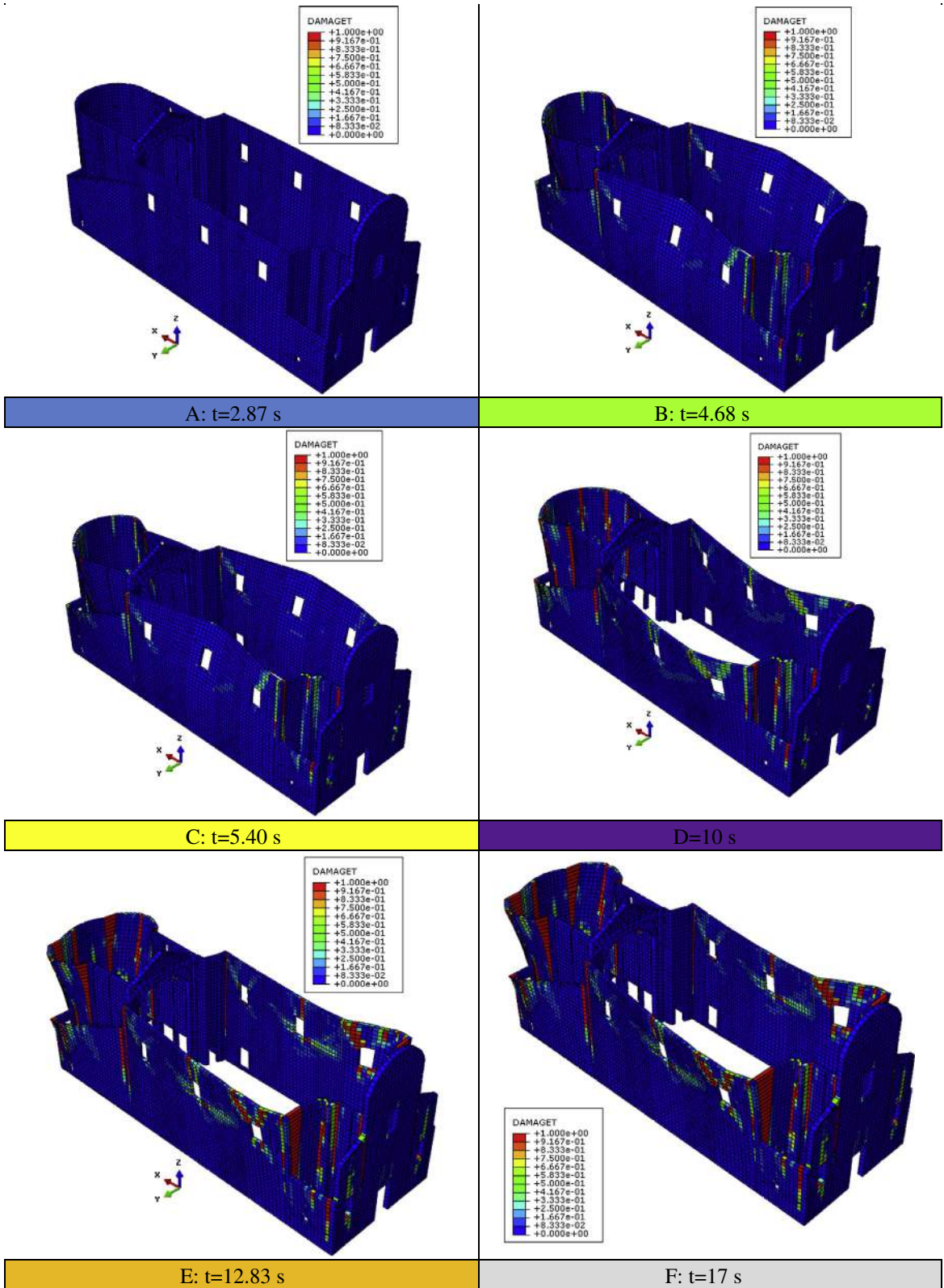


Fig. 30. Church 5. Seismic excitation in the transversal direction of the church. Deformed shape at different instants during the time-history with indication of damage (red, 1: full damage; blue, 0: no damage). (For interpretation of the references to color in this figure legend, the reader is referred to the web version of this article.)

approximate, because masonry exhibits a non-linear behavior even at very low levels of the external loads, such a standard approach may give a rough indication of the partial collapse mechanisms that can be compared with more sophisticated methods of analysis, such as non-linear static and dynamic approaches.

Pushover and limit analyses are more complex and obviously more realistic because they may partially or totally take into account some key features exhibited by masonry, such as the very low tensile strength, eventually the orthotropic behavior (if suitable FE codes are at disposal [18,19]), softening and damage in both tension and compression [23,24]. The output information provided is an estimation of both the collapse accelerations and the corresponding active failure mechanisms.

In this context, the present non-linear dynamic analyses, which may be reasonably considered as the highest level of complexity nowadays available in the framework of FE simulations, are assumed as reference to deduce useful indications to extend to different case studies showing similar geometrical features. The main quantitative and qualitative information that can be obtained from the results provided by the non-linear dynamic analyses performed in this study addresses the following issues: (1) individuation of the type of active failure mechanism (partial or global collapse, contour plots of damage, etc.) and corresponding collapse acceleration; (2) evaluation of the behavior factor; (3) effects of interlocking between perpendicular walls; (4) torsional effects and geometric irregularities; (5) influence of masonry compressive strength. Hereafter, all the above-mentioned issues are discussed in detail in order to deduce, from the large set of data obtained, some

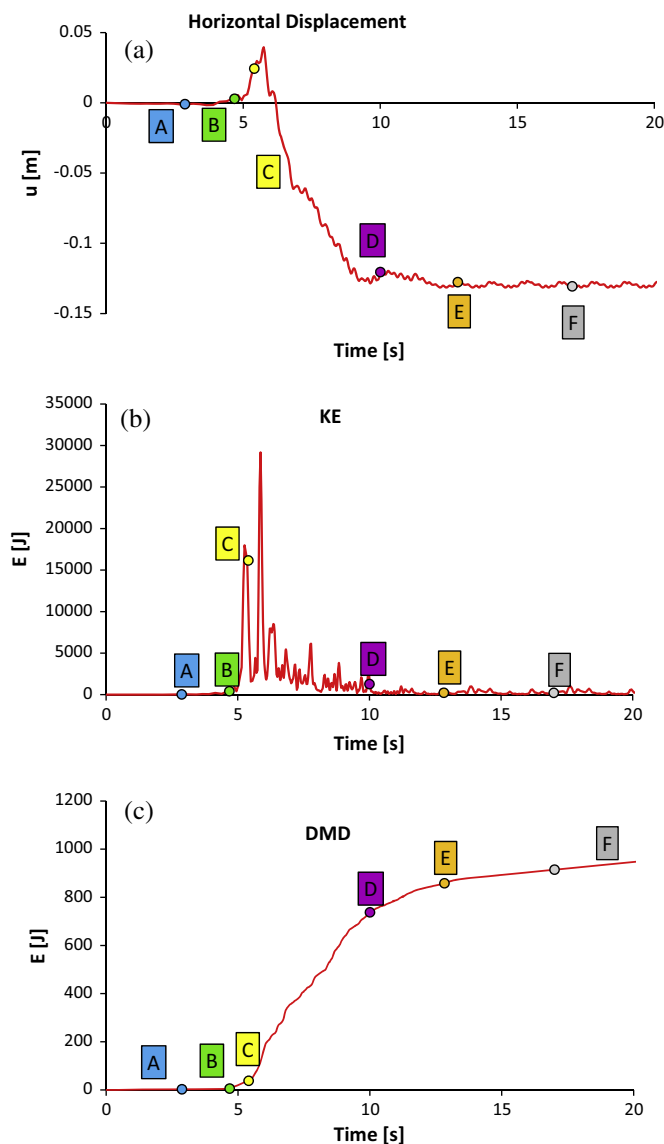


Fig. 31. Church 6. Seismic excitation in the longitudinal direction of the church. (a) Control point horizontal displacement time-history diagram. (b) Kinetic energy time-history diagram. (c) Energy dissipation in tension time-history diagram.

considerations about the comparative analyses performed to utilize in a more general framework. Moreover, a comparative synopsis of some results provided by the different approaches adopted is reported from Fig. 39 (Churches 1 and 2) to Fig. 42 (Church 7).

5.1. Information on the ultimate behavior

Non-linear dynamic analyses may provide useful information about the possible active failure mechanisms, residual displacements of a control node and peak ground acceleration corresponding to the collapse of the structure. Failure modes and collapse accelerations may be compared to put in evidence possible discrepancies among the different numerical approaches adopted.

In almost the totality of the cases, it is found that there is a qualitative satisfactory agreement among the results provided by the different analyses. In particular, the results provided by the present time-consuming non-linear dynamic simulations confirm, generally and at least from a qualitative point of view (i.e. prediction of the failure mechanisms and critical regions of damage), the output obtained by the static approaches. Despite these latter procedures, especially when dealing with limit analysis, are based on quite questionable hypotheses done on both mechanical properties and behavior of the materials, as well as on the application of the horizontal loads, it seems, from the comprehensive set of the simulations here provided, that they are able to identify the most critical portions of the structure needing seismic upgrading. From a detailed comparison among failure mechanisms obtained with the different analyses, it can be concluded that, according to Table 1, the most

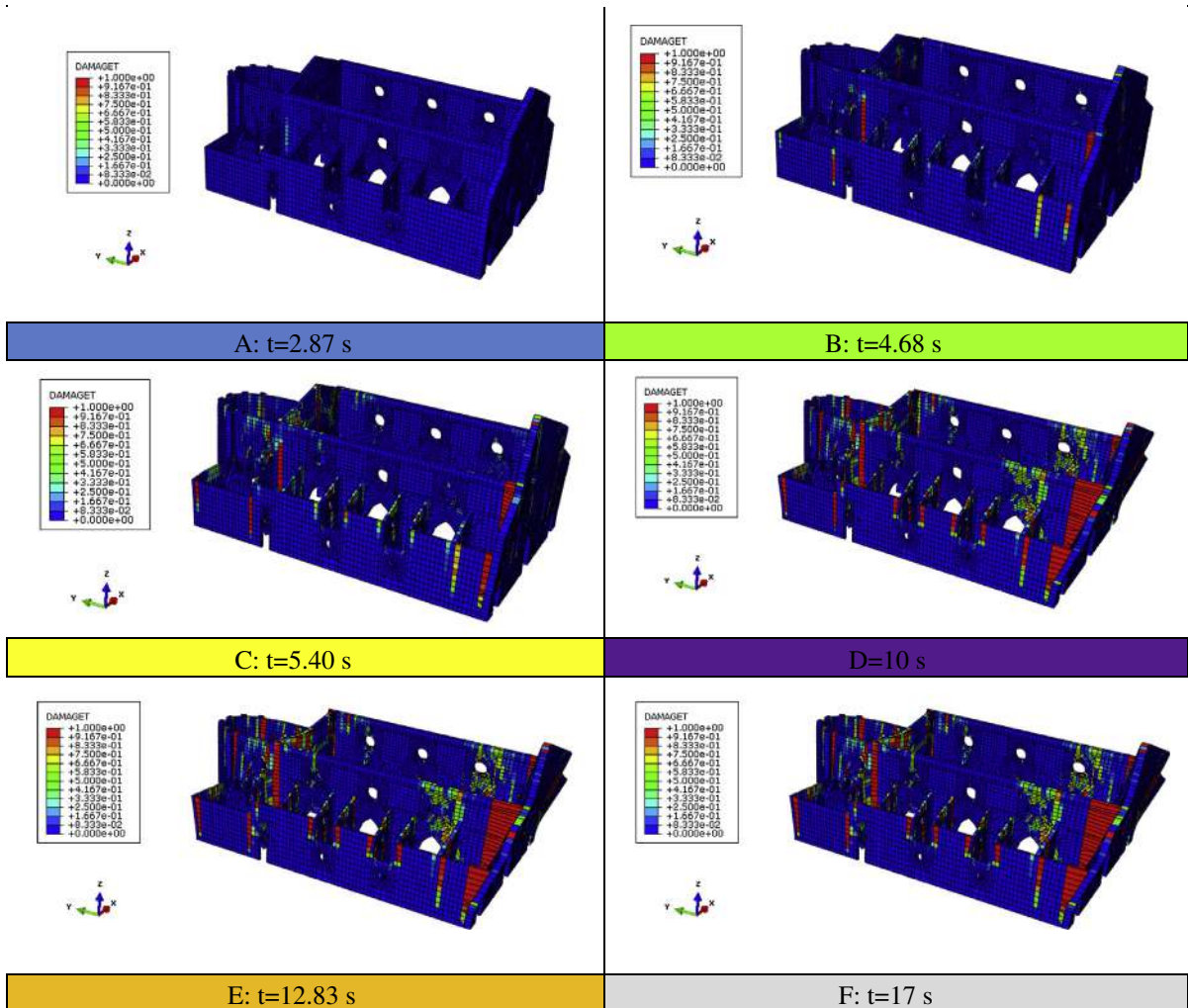


Fig. 32. Church 6. Seismic excitation in the longitudinal direction of the church. Deformed shape at different instants during the time-history with indication of damage (red, 1: full damage; blue, 0: no damage). (For interpretation of the references to color in this figure legend, the reader is referred to the web version of this article.)

vulnerable part of the churches under study is usually represented by the façade (either for the partial/global overturning or for the tympanum failure).

When the seismic action is applied in the transversal direction of the church, the out-of-plane failure of the long and slender lateral walls is almost always active at very low acceleration levels. In Church 2, the presence of stiffening pillars helps in enhancing the stability of the façade, also improving the interlocking with perpendicular walls. Crack patterns observed are indeed consistent with the formation of inclined yield lines spreading from the upper lateral zones.

When the seismic action is applied in the longitudinal direction of the church, apart the façade, other critical macro-blocks are the apse and the presbytery zones, which fail for a combination of shear and out-of-plane weaknesses, depending on the geometry (e.g. long and tall presbyteries are generally associated with shear damage). In several simulations, it has been observed that the non-linear dynamic analysis accurately reproduces the weakness of such parts, with crack patterns found at the end of the seismic excitations again in agreement with intuition.

5.2. Behavior factor

The behavior factor q for existing masonry buildings is still the object of scientific debate and therefore also the seismic design code provisions have not yet reached a general consensus. Italian Guidelines on the Built Heritage [28], a document which the NTC 2008 design Code [38,39] explicitly refers to, suggest that the value of the behavior factor should be selected between 1.5 and 3, depending on the characteristics of the masonry structure. The range is extremely large and highlights

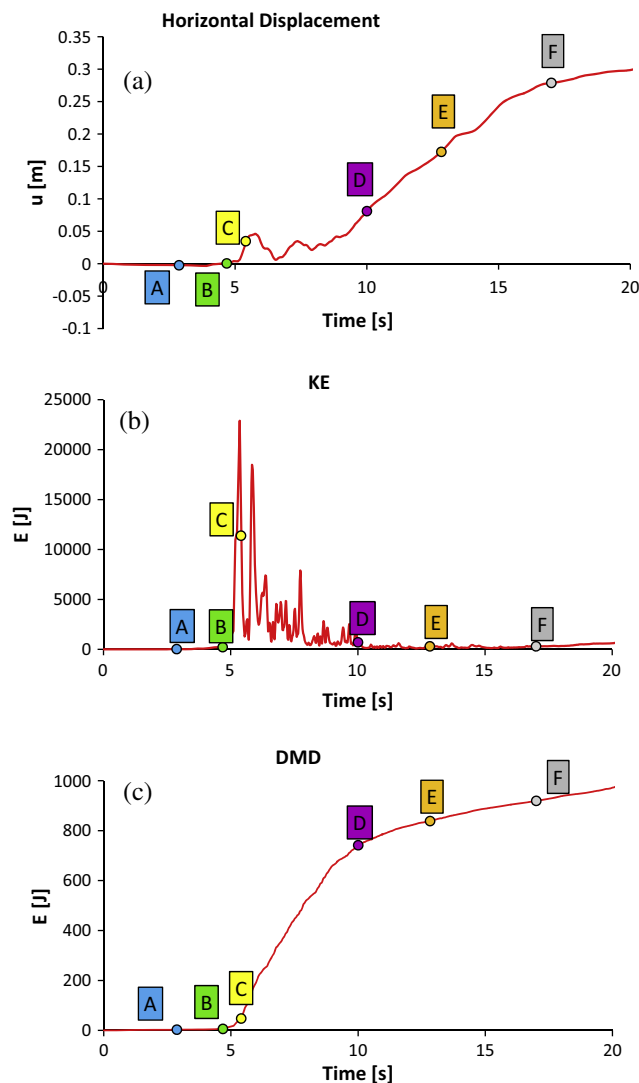


Fig. 33. Church 6. Seismic excitation in the transversal direction of the church. (a) Control point horizontal displacement time-history diagram. (b) Kinetic energy time-history diagram. (c) Energy dissipation in tension time-history diagram.

how the determination of the behavior factor is still a very difficult task for masonry structures. According to Brandonisio et al. [3], in absence of more precise data, it is suggested to assume the behavior factor q equal to 2.8, because it is the value of the behavior factor recommended by NTC 2008 for one-story unreinforced masonry buildings and it is within the range 1.5–3. Some other authors safely reduce the behavior factor q to 2.25, but a systematic analysis on this issue is still missing.

The non-linear dynamic analyses performed in the present paper can provide a cumbersome estimation of the behavior factor as follows:

- For each church and along both longitudinal and transversal directions, the accelerogram is applied to determine: (1) the PGA associated with the activation of the first failure mechanism; (2) the PGA inducing a first plasticization – or first damage – on the active failure mechanism. The non-linear dynamic analyses should be repeated using different scaling factors to modify the PGA of the strong ground motion.
- The estimation of first damage is not an easy task for existing masonry structures. In this study it was determined quantitatively, plotting the evolution of damage in tension, as done for example for Church 1 in Fig. 10c, and evaluating the cumulated damage at the end of the seismic event. If the cumulated damage is sufficiently small but non-zero, then it can be reasonably stated that the point of first plasticization (damage) is reached.

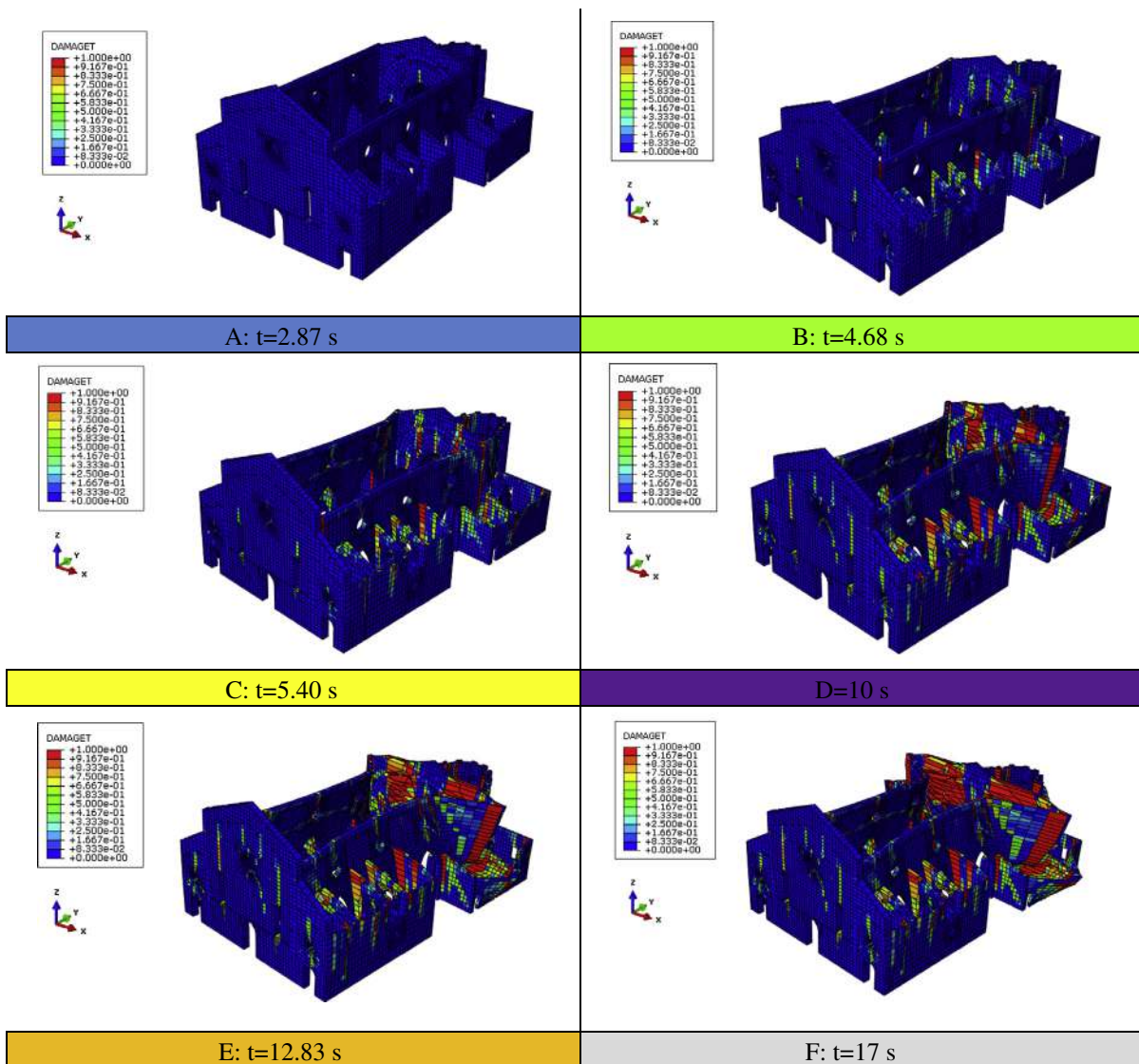


Fig. 34. Church 6. Seismic excitation in the transversal direction of the church. Deformed shape at different instants during the time-history with indication of damage (red, 1: full damage; blue, 0: no damage). (For interpretation of the references to color in this figure legend, the reader is referred to the web version of this article.)

- The procedure is iterative because the scaling factor of the strong ground motion is not a-priori known. Typically a classic bisection procedure is adopted, bounding more and more strictly at each iteration the target scaling factor. Normally the scaling factor is bracketed sufficiently well in no more than five iterations.

It is worth mentioning that the procedure proposed is approximate and requires further validations, especially changing the accelerogram adopted. Different accelerograms (either real or spectrum-compatible) should be used, with a statistical treatment of the results obtained. The work is comprehensive and is still in progress; it will be therefore presented in due course in a dedicated publication, exclusively focusing on such specific issue [49].

A comparison between the behavior factors obtained by means of non-linear dynamic analyses and those evaluated by means of pushover analyses is reported in Table 2. As can be noted, non-linear dynamic analyses systematically provide smaller values of the behavior factor. While there may be many reasons for this result, the most important is likely the material model adopted in the dynamic analyses, which exhibits damage. On the contrary, an elastic-perfectly plastic behavior is assumed within the pushover approach [11]. Intuitively, a material model with damage reduces the capacity of the structure to dissipate beyond the elastic limit, at least in comparison with a material that does not exhibit softening.

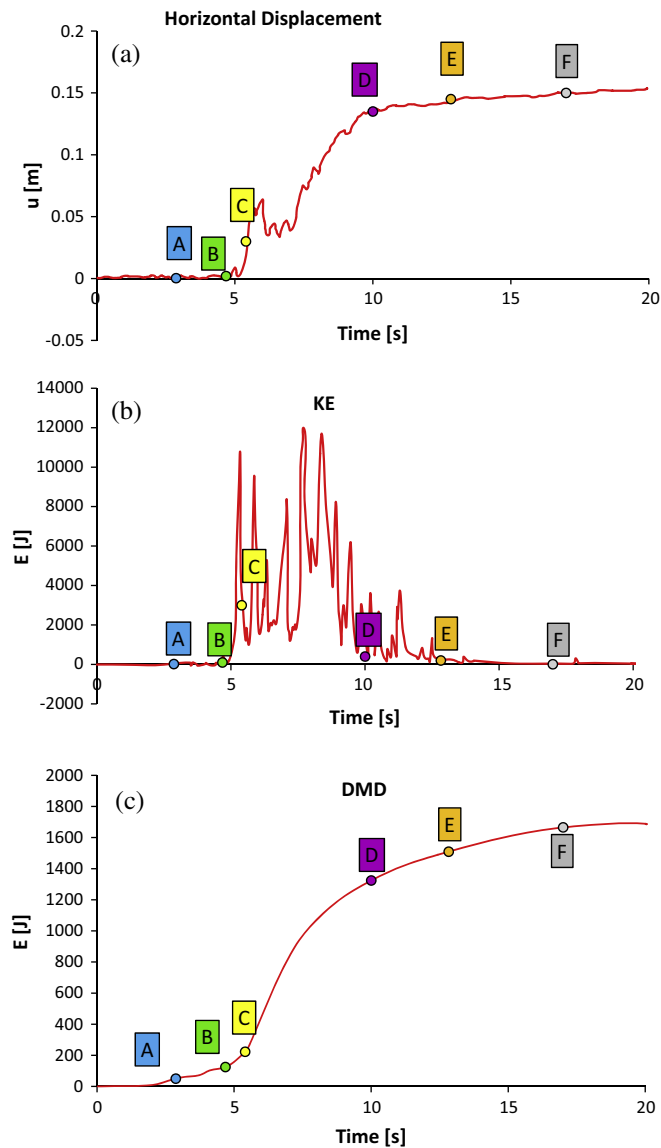


Fig. 35. Church 7. Seismic excitation in the longitudinal direction of the church. (a) Control point horizontal displacement time-history diagram. (b) Kinetic energy time-history diagram. (c) Energy dissipation in tension time-history diagram.

5.3. Interlocking between perpendicular walls

Interlocking between perpendicular walls may play a crucial role in the increase of the load bearing capacity of a single macro-element and on a change of the failure the failure mechanism. In addition, it has a strong influence on the determination of the behavior factor of the structure. When interlocking is absent, for instance when the failure mechanism of a wall is represented by the overturning around a horizontal hinge, then the instant of formation of the hinge corresponds by definition to the activation of the failure mechanism and the behavior factor is rigorously equal to 1. Moreover, it is worth mentioning that, due to the very low masonry tensile strength, the load bearing capacity against horizontal actions is almost all secured by gravity loads. Therefore, the contribution of interlocking between perpendicular walls may help in dissipating energy in correspondence of the connection and hence may have an influence on the increase of the collapse acceleration, in some cases with a substantial change of the failure mechanism and the formation of inclined yield lines.

Unfortunately, the correct evaluation of interlocking effectiveness is almost always very difficult and in the majority of the cases cannot be done with sufficient accuracy, even after in-situ surveys. A suitable brick pattern with good mechanical properties of the mortar joints and the presence of tie rods may considerably increase its effectiveness. Conversely, authors experienced that FE models with macro-blocks assumed as not linked with neighboring walls at the vertical edges turned out to be extremely vulnerable to horizontal actions, showing unrealistically low values of collapse accelerations. In the present simulations, therefore, perpendicular walls are assumed as connected node by node, but the mechanical properties assumed

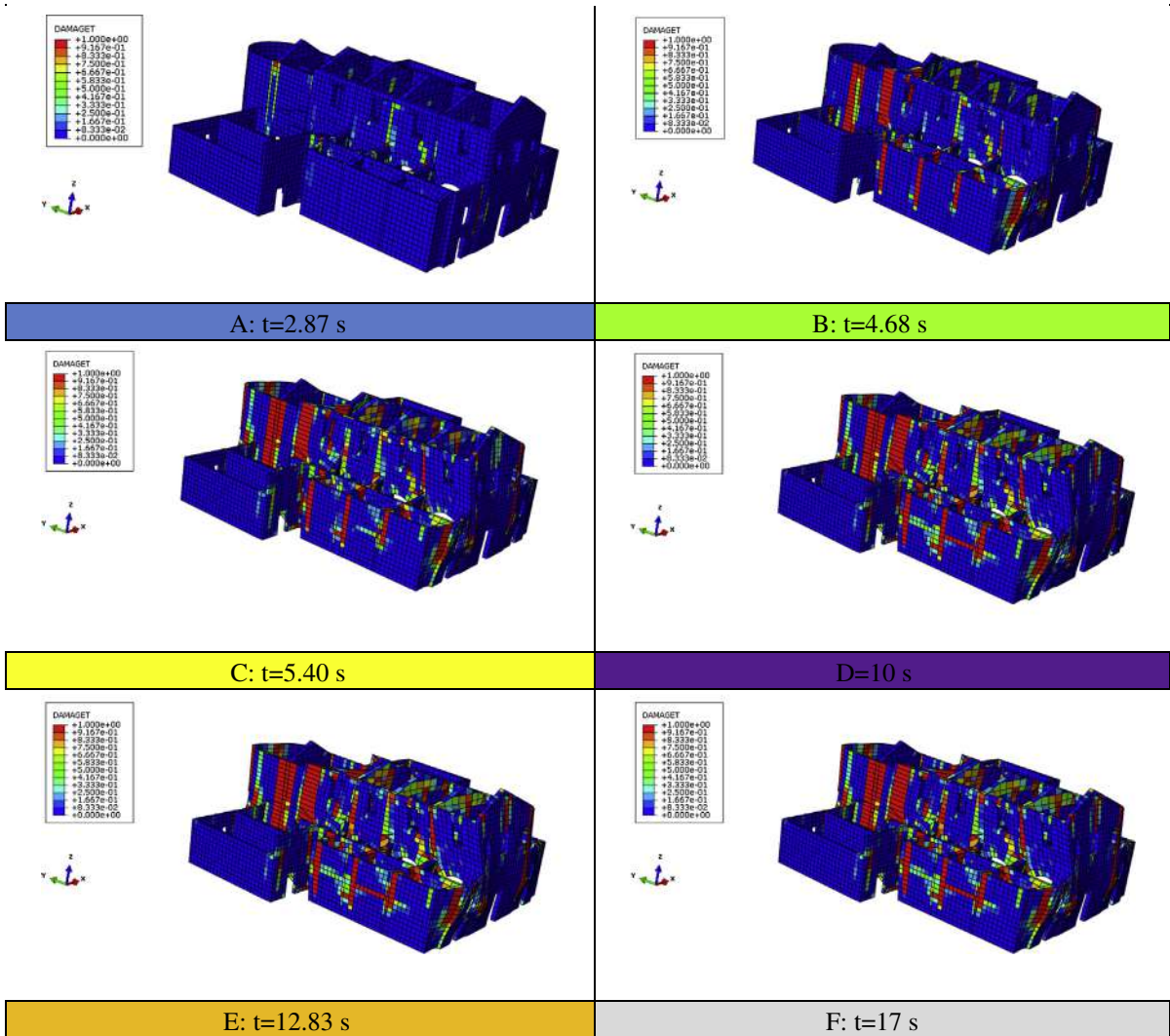


Fig. 36. Church 7. Seismic excitation in the longitudinal direction of the church. Deformed shape at different instants during the time-history with indication of damage (red, 1: full damage; blue, 0: no damage). (For interpretation of the references to color in this figure legend, the reader is referred to the web version of this article.)

for the interfaces shared by contiguous walls are extremely low (the same used for the surrounding masonry), especially in tension. It is therefore reasonable to state that the beneficial contribution provided by interlocking is still very moderate. In almost all the cases, the activation of the failure mechanism occurs similarly to the cases where interlocking is neglected (e.g. overturning of the façade), but with higher failure accelerations. The resultant behavior factor is higher than one but lower than that recommended by Italian code.

5.4. Torsional effects

Analyzing in detail the numerical results obtained from non-linear dynamic analyses, it is worth noting that torsional effects due to earthquake motions are generally variable for the different churches investigated and may play a crucial role in some situations where asymmetries and irregularities are present. For Church 2 and Church 4 undesirable torsional effects are slightly more evident, because the bell tower embedded into the church plan represents a strong irregularity for both horizontal stiffness and mass distribution. All other cases exhibit a response with small torsional effects, especially along the longitudinal direction, even at significant levels of damage, i.e. near the activation of a partial failure mechanism. For

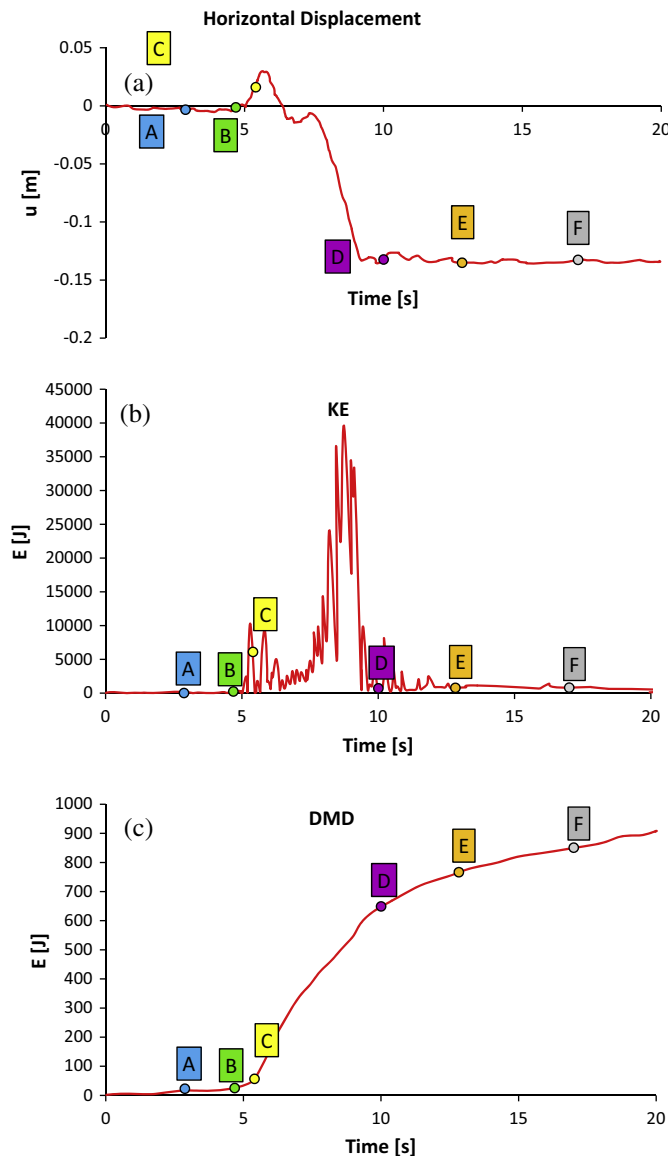


Fig. 37. Church 7. Seismic excitation in the transversal direction of the church. (a) Control point horizontal displacement time-history diagram. (b) Kinetic energy time-history diagram. (c) Energy dissipation in tension time-history diagram.

Church 2 and Church 4, the behavior factors evaluated through non-linear dynamic analyses are obviously lower than those obtained using pushover analyses, but not considerably lower than those found in different cases with negligible torsional effects. As a consequence, it is authors' opinion that the discrepancies observed for the values of the behavior factor between non-linear static and dynamic approaches are more a consequence of the different material models adopted rather than of possible torsional effects. The active failure mechanisms, indeed, are very similar to those found for the almost symmetric cases (e.g. façade failure, perimeter walls collapse, etc.).

A final remark regarding geometric irregularities should be made with reference to double curvature masonry structures, as cross-vaults and domes [50]. Such structural elements are traditionally conceived to withstand vertical loads, but their role under horizontal actions is still an open issue and should be quantified with particular care. At present, reliable simplified models are still missing but, intuitively, it can be stated that the presence of vaulted structure may increase the box behavior, at the same time increasing the seismic mass and representing a not negligible cause of in-plan irregularity when they are concentrated only in specific zones (as for instance for Church 6, where vaults are present only in the presbytery/

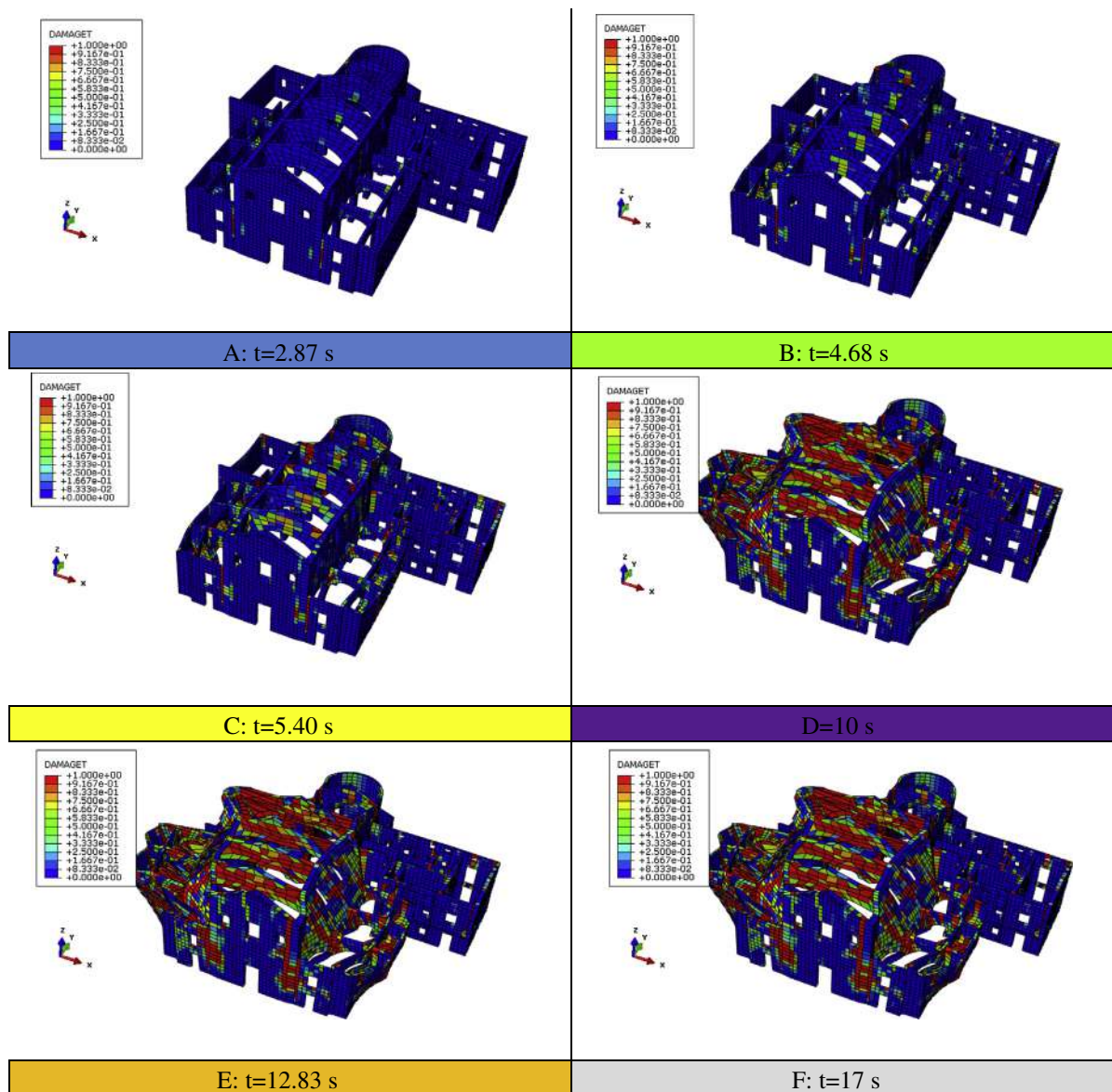


Fig. 38. Church 7. Seismic excitation in the transversal direction of the church. Deformed shape at different instants during the time-history with indication of damage (red, 1: full damage; blue, 0: no damage). (For interpretation of the references to color in this figure legend, the reader is referred to the web version of this article.)

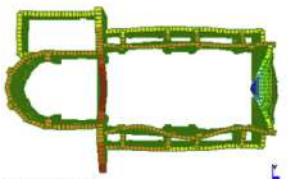
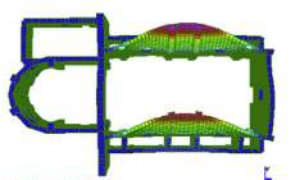
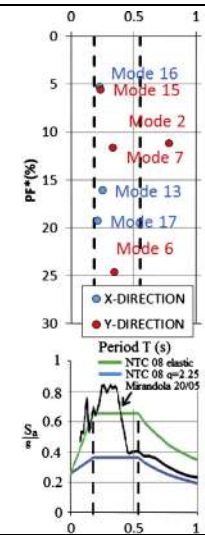
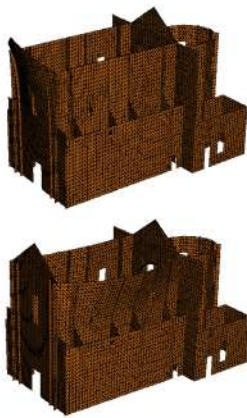
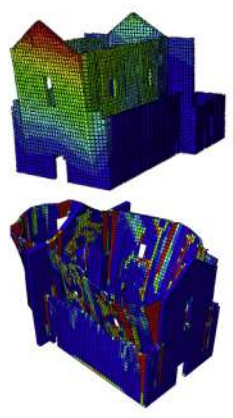
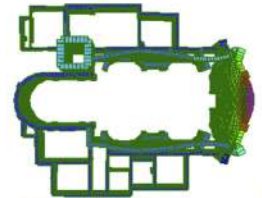
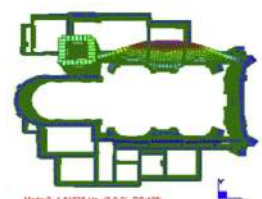
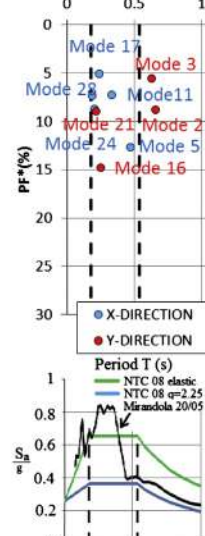

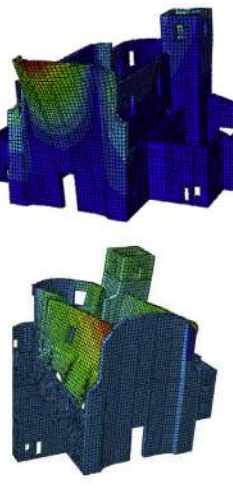
Conventional eigen-frequency analysis		FE limit analysis/pushover	Non-linear dynamic analysis
Church 1	Period/participating mass	Collapse acceleration	Residual displacement
Longitudinal direction	0.25 s / 16%	0.05g / 0.05g	300 mm
Transversal direction	0.78 s / 11%	0.06g / 0.075g	120 mm
<p>Mode 13</p>  <p>Mode 2</p> 			
Church 2	Period/participating mass	Collapse acceleration	Residual displacement
Longitudinal direction	0.48 s / 13%	0.047g / 0.055g	100 mm
Transversal direction	0.6 s / 10%	0.041g / 0.042g	80 mm
<p>Mode 5</p>  <p>Mode 2</p> 			

Fig. 39. Churches 1 and 2. Seismic excitation in the longitudinal and transversal direction of the church. Comparison of the structural behavior by means of different approaches.

apse). For the cases analyzed, only Church 6 presents vaulted structures. For this reason, it appears difficult to draw conclusive considerations on this issue.

5.5. Masonry compressive strength

It has been proved, through many experimental tests conducted after the 2012 seismic event, see for instance [51], that in the region hit by the earthquake historical masonries exhibit quite good mechanical properties in compression, secured by high values of resistance of the clay bricks. It is indeed common opinion that the surprisingly low load bearing capacity of

Table 1

Active failure mechanisms derived from the different analyses performed.

Church		Non-linear dynamic analysis	Pushover analysis	FE limit analysis	Kinematic limit analysis with pre-assigned failure mechanisms
1	1 longitudinal	Façade (base yield line) Lateral walls (shear) Triumphal arch (out-of-plane)	Façade tympanum (inclined yield line)	Façade tympanum (inclined yield line)	F2: Façade overturning (middle height yield line)
	1 transversal	Lateral walls (out-of-plane) Triumphal arch (shear) Apse (out-of-plane)	Lateral walls (out-of-plane)	Lateral walls (out-of-plane)	A2: Lateral walls failure (internal)
2	2 longitudinal	Façade (inclined yield lines, upper part) Bell tower	Façade (upper part)	Façade tympanum (almost horizontal yield line)	F2: Façade overturning (middle height yield line)
	2 transversal	Lateral walls (out-of-plane failure) Apse	Lateral wall near bell tower (out-of-plane failure)	Lateral wall near bell tower (out-of-plane failure)	A2: Lateral walls failure (internal)
3	3 longitudinal	Façade (middle height hinge)	Façade with portion transversal walls central nave	Façade tympanum (almost horizontal yield line)	F2: Façade overturning (middle height yield line)
	3 transversal	Lateral walls (detachment and overturning)	Transect portion (out-of-plane and shear)	Lateral walls (detachment and overturning)	A1: Lateral walls failure (external)
4	4 longitudinal	Façade (vertical yield line, detachment from perp. walls)	Façade tympanum (horizontal yield line)	Façade tympanum (horizontal yield line)	F2: Façade overturning (middle height yield line)
	4 transversal	Central nave lateral walls (out-of-plane failure) Triumphal arch (shear)	Central nave lateral walls (out-of-plane failure)	Central nave lateral walls (out-of-plane failure)	A1: Lateral walls failure (external)
5	5 longitudinal	Façade (base hinge)	Façade tympanum (horizontal yield line)	Façade tympanum (horizontal yield line)	F2: Façade overturning (middle height yield line)
	5 transversal	Single nave lateral walls (out-of-plane failure)	Single nave lateral walls (out-of-plane failure)	Single nave lateral walls (out-of-plane failure)	A1: Lateral walls failure (external)
6	6 longitudinal	Façade (base hinge)	Façade (upper part, inclined yield lines)	Façade (middle horizontal hinge)	F2: Façade overturning (middle height yield line)
	6 transversal	Triumphal arch (in-plane shear) Central nave walls (out-of-plane failure) Apse (shear & out-of-plane)	Central nave walls (out-of-plane failure)	Central nave walls (out-of-plane failure), Apsse (out-of-plane) Triumphal arch (in-plane shear, not totally active)	A2: Lateral walls failure (internal)
7	7 longitudinal	Façade (partial out-of-plane) Central nave walls (shear)	Façade and longitudinal walls (shear, global)	Façade (upper part, inclined yield lines)	F1: Façade overturning (base yield line)
	7 transversal	Transversal stiffening arches (shear) Lateral walls central nave (out-of-plane failure)	Lateral chapels and central nave longitudinal walls (global)	Stiffening arches (shear), lateral walls central nave (out-of-plane failure)	A2: Lateral walls failure (internal)

Table 2

Evaluation of the behavior factor for the churches analyzed by means of the present non-linear dynamic analyses and non-linear static pushover approach.

Church	Non-linear dynamic analyses		Pushover analyses	
	Longitudinal direction	Transversal direction	Longitudinal direction	Transversal direction
1	1.86	1.92	2.56	2.84
2	1.32	1.44	2.05	2.46
3	2.20	2.15	2.71	2.24
4	1.31	1.89	1.57	1.74
5	1.77	1.94	2.92	1.81
6	2.01	2.34	2.16	2.36
7	1.97	1.81	2.13	2.11

towers and churches in the area is due more to the deterioration of mortar joints (and hence their almost vanishing tensile strength) rather than to crushing of the bricks in compression. It would be therefore unrealistic to perform sensitivity analyses reducing the compressive strength up to the activation of damage and plastic dissipation in compression. Such a contribution, in terms of cumulated dissipated energy, would be at least one order of magnitude higher than that registered in tension, with clear incorrect estimations of collapse accelerations associated with unrealistic failure mechanisms. When moderate values of compressive strength are adopted in the non-linear dynamic simulations (as those used in the present paper), authors experienced a negligible contribution of non-linearity in compression, once again confirming the

intuitive thought that the behavior of such typology of structures is driven by the low tensile strength and the stabilizing effect of the self weight.

Finally, the following considerations about the standard eigen-frequency analysis may be drawn from Figs. 39–42:

(A) The first two modes characterized by not negligible participating mass generally exhibit a period T ranging between 0.2 and 0.4 s.

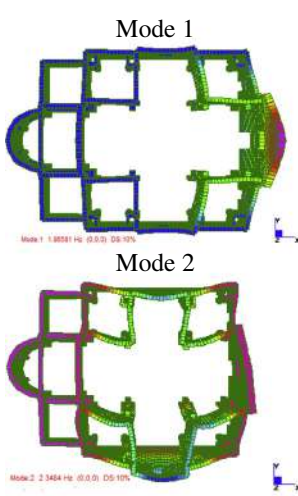
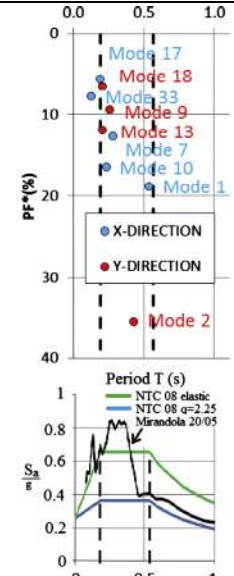
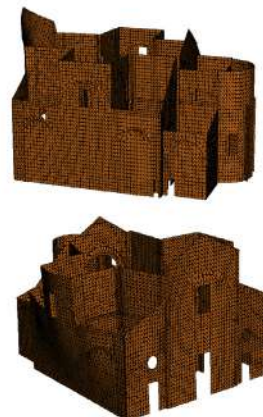
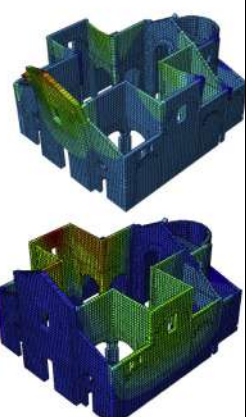
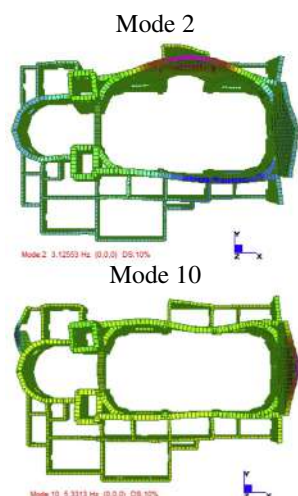
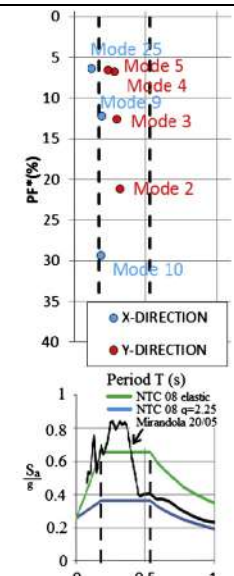
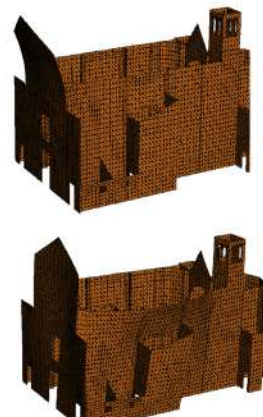
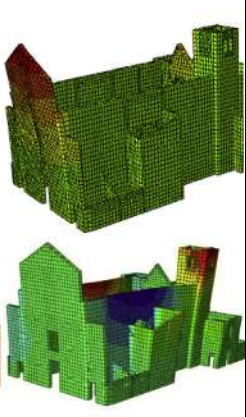
Conventional eigen-frequency analysis		FE limit analysis/pushover	Non-linear dynamic analysis
Church 3	Period/participating mass	Collapse acceleration	Residual displacement
Longitudinal direction	0.25 s / 16%	0.12g / 0.085g	120 mm
Transversal direction	0.78 s / 11%	0.072g / 0.075g	60 mm
 <p>Mode 1 Mode 2</p>	 <p>PF (%)</p> <p>Period T (s)</p>		
Church 4	Period/participating mass	Collapse acceleration	Residual displacement
Longitudinal direction	0.48 s / 13%	0.039g / 0.041g	110 mm
Transversal direction	0.6 s / 10%	0.078g / 0.084g	60 mm
 <p>Mode 2 Mode 10</p>	 <p>PF (%)</p> <p>Period T (s)</p>		

Fig. 40. Churches 3 and 4. Seismic excitation in the longitudinal and transversal direction of the church. Comparison of the structural behavior by means of different approaches.

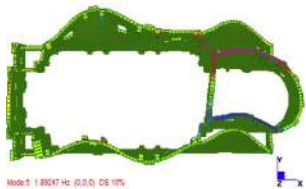
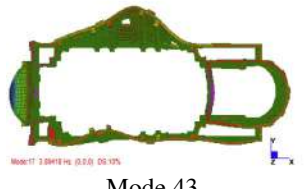

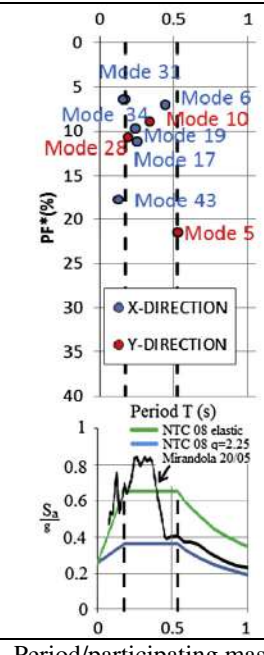

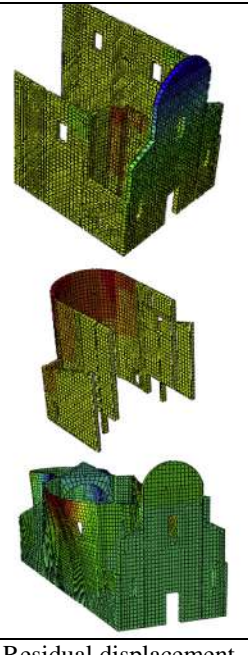

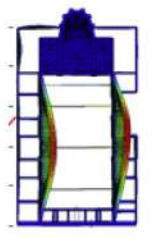
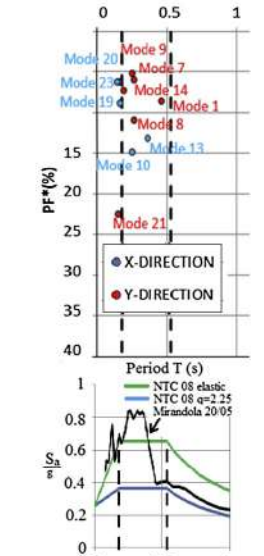
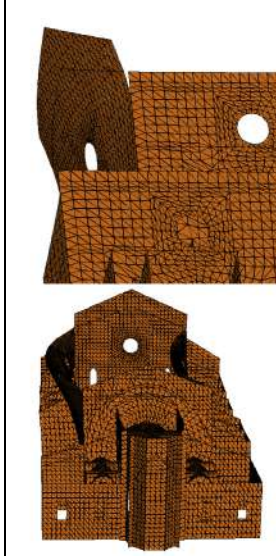
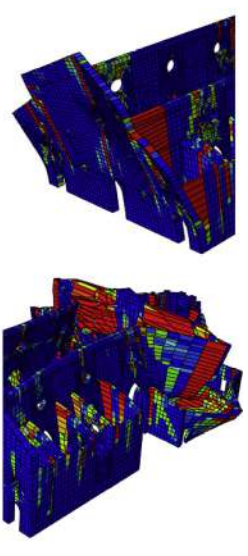
Conventional eigen-frequency analysis		FE limit analysis/pushover	Non-linear dynamic analysis
Church 5	Period/participating mass	Collapse acceleration	Residual displacement
Longitudinal direction	0.132 s / 18%	0.077g / 0.034g	120 mm
Transversal direction	0.529 s / 22%	0.092g / 0.088g	70 mm
Mode 5  Mode 17  Mode 43 			
Church 6	Period/participating mass	Collapse acceleration	Residual displacement
Longitudinal direction	0.25 s / 15%	0.067g / 0.044g	140 mm
Transversal direction	0.195s / 22.5%	0.048g / 0.045g	300 mm
Mode 21  Mode 2 			

Fig. 41. Churches 5 and 6. Seismic excitation in the longitudinal and transversal direction of the church. Comparison of the structural behavior by means of different approaches.

(B) The deformed shapes associated with the first two modes with not negligible participating mass are local, mainly representing either a partial (tympanum or middle height) or global overturning of the façade in the longitudinal direction or two-way bending of the long lateral walls in the transversal direction. When damage starts to occur, the elastic periods so found are not realistic anymore and this is the major theoretical limitation of a standard

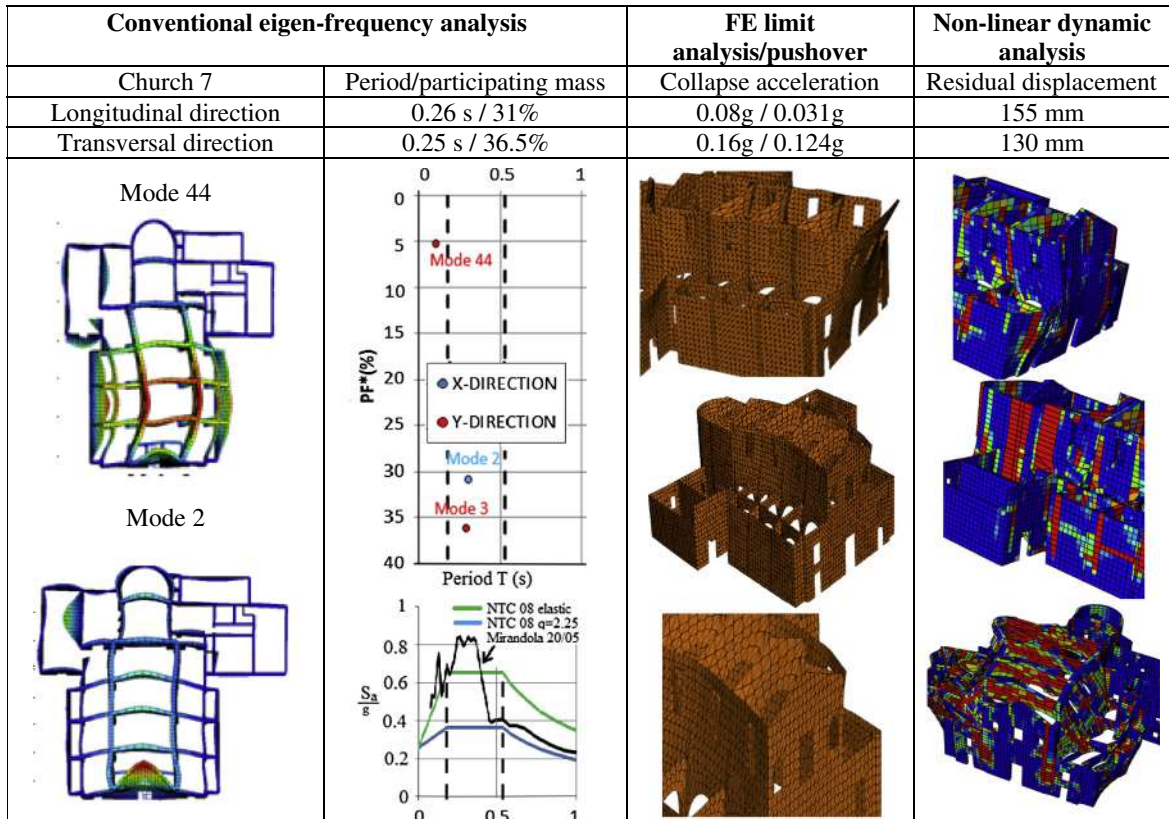


Fig. 42. Church 7. Seismic excitation in the longitudinal and transversal direction of the church. Comparison of the structural behavior by means of different approaches.

response spectrum analysis. It can be therefore reasonably stated that a standard eigen-frequency analysis may only give a rough initial indication of the most critical failure mechanisms that are likely to occur for churches subjected to seismic excitations.

6. Conclusions

In the present paper seven masonry churches damaged by the 2012 Emilia Romagna (Italy) seismic sequence have been analyzed numerically. Non-linear dynamic analyses have been performed using a real accelerogram registered near the epicenter of one of the shakes (Mirandola) and applied, separately, in both the longitudinal and transversal directions. A smeared crack damage-plasticity isotropic softening material has been used to model masonry, which typically exhibits very low tensile strength and softening in tension.

The final aim of the numerical investigation carried out in this study is to put at disposal the results of a sensitivity analysis conducted on a sufficiently large sample in order to establish if the simplifications assumed in common design may be always regarded as reliable or if discrepancies exist. To this aim, the reference solution has been reasonably considered that provided by the non-linear dynamic analyses. A variety of alternative procedures, ranging from simple (as for instance response spectrum analyses and kinematic limit analyses with pre-assigned failure mechanisms) to moderate/difficult (non-linear static analyses and FE limit analyses) approaches, has been critically applied and the results compared. The need to analyze several different case studies derives from the peculiar characteristics of masonry churches, the most important being the very large geometric variability and irregularity, as well as the architectural complexity.

From an overall analysis of the results obtained, the following remarks may be made:

- Standard eigen-frequency analyses associated with code response spectra may help to roughly identify the possible macro-blocks that could cause collapse during a seismic event. However such analysis becomes unreliable when masonry is loaded beyond the elastic limit. Since masonry tensile strength is always very low, even small PGAs may cause damage. Therefore the results provided by standard eigen-frequency analyses should be considered with care.
- The evaluation of collapse accelerations by means of pre-assigned failure mechanisms is very sensitive to the hypotheses done on interlocking between perpendicular walls, providing very conservative results in the majority of the cases. As a

rule, the failure mechanism is correctly identified in presence of simple case studies without irregularities, but the peculiarity of the different case studies (e.g. presence of buttresses, internal cross vaults, non standard geometries, openings, etc.) is sometimes lost. The macro-blocks that are critical with a significantly higher occurrence are represented by the façade and the lateral walls.

- Limit analysis combined with a detailed FE discretization and pushover analysis have proved to be able to capture the failure mechanisms with a more accurate detail, and to reproduce case by case the geometric specificity of each church. Despite the large amount of approximations introduced with a static approach and the simplified material models assumed for masonry (e.g. rigid perfectly plastic model with associated flow rule in limit analysis, isotropic elastic-plasticity for pushover analyses), collapse accelerations and active failure mechanisms seem in reasonable agreement with refined time-consuming non-linear dynamic simulations.
- The behavior factors evaluated through pushover analyses are systematically higher than those provided by non-linear dynamic analyses, but the role played by geometric irregularities and mass eccentricities causing torsion seems to be less crucial than the material model adopted in the computations. The behavior factor provided by Italian code appears probably overestimated for such typologies of structures.

The sensitivity study conducted allows stating that the seismic vulnerability of such complex structures should be always evaluated through different procedures, including standard eigen-frequency approaches, limit and non-linear static analyses. Indeed, all the aforementioned strategies are affected by different levels of accuracy and complexity, but, if performed together, may provide a convincing picture of the structural weakness, at least when the study by means of non-linear dynamic analyses is not possible either for time and software limitations or for insufficient experience of the user.

Acknowledgements

This work has been carried out within a research agreement between Politecnico di Milano and Curia di Ferrara, under the scientific responsibility of Prof. Gabriele Milani (Politecnico) and Eng. Don Stefano Zanella (Curia), who is gratefully acknowledged by the authors. Part of the analyses were developed within the activities of Rete dei Laboratori Universitari di Ingegneria Sismica – ReLUIS for the research program funded by the Dipartimento di Protezione Civile – Progetto Esecutivo 2014.

References

- [1] Dogliani F, Moretti A, Petrini V. Le chiese e il terremoto. Edizioni LLINT, Trieste, Italy; 1994 [Churches and earthquake].
- [2] Parisi F, Augusti N. Earthquake damages to cultural heritage constructions and simplified assessment of artworks. *Eng Fail Anal* 2013;34:735–60.
- [3] Brandonisio G, Lucibello G, Mele E, De Luca A. Damage and performance evaluation of masonry churches in the 2009 L'Aquila earthquake. *Eng Fail Anal* 2013;34:693–714.
- [4] Foraboschi P. Church of San Giuliano di Puglia: seismic repair and upgrading. *Eng Fail Anal* 2013;33:281–314.
- [5] Bartoli G, Betti M. Cappella dei Principi in Firenze, Italy: experimental analyses and numerical modeling for the investigation of a local failure. *J Perform Constr Facil* 2013;27(1):4–26.
- [6] Betti M, Bartoli G, Orlando M. Evaluation study on structural fault of a Renaissance Italian palace. *Eng Struct* 2010;32(7):1801–13.
- [7] Fregonese L, Barbieri G, Biolzi L, Bocciarelli M, Frigeri A, Taffurelli L. Surveying and monitoring for vulnerability assessment of an ancient building. *Sensors (Switzerland)* 2013;13(8):9747–73.
- [8] Barbieri G, Biolzi L, Bocciarelli M, Fregonese L, Frigeri A. Assessing the seismic vulnerability of a historical building. *Eng Struct* 2013;57:523–35.
- [9] Pieraccini M, Dei D, Betti M, Bartoli G, Tucci G, Guardini N. Dynamic identification of historic masonry towers through an expeditious and no-contact approach: application to the “Torre del Mangia” in Siena (Italy). *J Cult Herit* 2014;15(3):275–82.
- [10] Fieni C, Mantovani A. Comportamento sismico delle chiese in muratura, analisi di 5 chiese dopo il sisma del Maggio 2012 in Emilia-Romagna. MSc Thesis, Technical University of Milan, Italy; 2013 [Seismic behavior of masonry churches. Analysis of 5 churches after the Emilia-Romagna, May 2012, earthquake].
- [11] Milani G, Valente M. Comparative pushover and limit analyses on seven masonry churches damaged by the 2012 Emilia-Romagna (Italy) seismic events: possibilities of non-linear finite elements compared with pre-assigned failure mechanisms. *Eng Fail Anal* 2015;47:129–61.
- [12] Giuffrè A, editor. Safety and conservation of historical centers: the Ortigia case. Roma – Bari: Laterza Press; 1993.
- [13] Lagomarsino S, Resemini S. The assessment of damage limitation state in the seismic analysis of monumental buildings. *Earthquake Spectra* 2009;25(2):323–46.
- [14] Lagomarsino S, Podestà S. Metodologie per l'analisi di vulnerabilità delle chiese. Atti del IX Convegno Nazionale “L'Ingegneria Sismica in Italia”. Torino 20–23 Settembre 1999 [Methodologies for the vulnerability analysis of churches].
- [15] Ordinanza n° 83 del 5 Dicembre 2012. Riparazione con rafforzamento locale e ripristino con miglioramento sismico degli edifici religiosi (chiese) [Rehabilitation with local strengthening and seismic upgrading of religious structures (churches)].
- [16] Lourenço PB, Roque JA. Simplified indexes for the seismic vulnerability of ancient masonry buildings. *Constr Build Mater* 2006;20:200–8.
- [17] Roque JA. Strengthening and structural rehabilitation of old masonry walls (in Portuguese)/Reforço e reabilitação estrutural de paredes antigas de alvenaria. MSc thesis, Universidade do Minho; 2002.
- [18] Milani G, Venturini G. Automatic fragility curve evaluation of masonry churches accounting for partial collapses by means of 3D FE homogenized limit analysis. *Comput Struct* 2011;89:1628–48.
- [19] Milani G, Venturini G. Safety assessment of four masonry churches by a plate and shell FE non-linear approach. *J Perform Constr Facil* 2013;27(1):27–42.
- [20] Milani G. Lesson learned after the Emilia Romagna, Italy, 20–29 May 2012 earthquakes: a limit analysis insight on three masonry churches. *Eng Fail Anal* 2013;34:761–78.
- [21] Augusti G, Ciampoli M, Zanobi S. Bounds to the probability of collapse of monumental buildings. *Struct Saf* 2002;24:89–105.
- [22] Augusti G, Ciampoli M, Giovenale P. Seismic vulnerability of monumental buildings. *Struct Saf* 2001;23:253–74.
- [23] Brandonisio G. Analisi di edifici a pianta basilicale soggetti ad azioni sismiche. PhD thesis, II University of Naples, Italy; 2007 [Analysis of structures with basilica plan subjected to seismic actions].

- [24] Giordano A. Sulla capacità sismica delle chiese a pianta basilicale. PhD thesis, University of Naples Federico II, Italy; 2001 [On the seismic capacity of churches with basilica plan].
- [25] Devaux M. Seismic vulnerability of cultural heritage buildings in Switzerland. PhD thesis, EPFL Lausanne, Switzerland; 2008.
- [26] Gattulli V, Antonacci E, Vestroni F. Field observations and failure analysis of the Basilica S. Maria di Collemaggio after the 2009 L'Aquila earthquake. *Eng Fail Anal* 2013;34:715–34.
- [27] Araujo A, Lourenço PB, Oliveira D, Leite J. Seismic assessment of St James Church by means of pushover analysis – before and after the New Zealand earthquake. *Open Civ Eng J* 2012;6:160–72.
- [28] DPCM 9/2/2011. Linee guida per la valutazione e la riduzione del rischio sismico del patrimonio culturale con riferimento alle Norme tecniche delle costruzioni di cui al decreto del Ministero delle Infrastrutture e dei trasporti del 14 gennaio; 2008 [Italian guidelines for the evaluation and the reduction of the seismic risk for the built heritage, with reference to the Italian norm of constructions].
- [29] Krabbenhoft K, Lyamin A, Krabbenhoft J. Optum CE; 2013. <<http://www.optumce.com/>>.
- [30] Gilbert M. Ring: a 2D rigid block analysis program for masonry arch bridges. In: Proc 3rd international arch bridges conference. Paris, France; 2001. p. 109–18.
- [31] Valente M. Seismic upgrading strategies for non-ductile plan-wise irregular R/C structures. *Procedia Eng* 2013;54:539–53.
- [32] Valente M. Seismic response of steel buildings with different structural typology. *Appl Mech Mater* 2013;256–259:2234–9.
- [33] Valente M. Seismic strengthening of non-ductile R/C structures using infill wall or ductile steel bracing. *Adv Mater Res* 2013;602–604:1583–7.
- [34] Valente M. Seismic rehabilitation of a three-storey R/C flat-slab prototype structure using different techniques. *Appl Mech Mater* 2012;193–194:1346–51.
- [35] Iervolino I, Chioccarelli E, De Luca F. Preliminary study of Emilia (May 20th 2012) earthquake ground motion records. Reluis report V2.11 2012. <<http://www.reluis.it>>.
- [36] Iervolino I, Chioccarelli E, De Luca F. Engineering seismic demand in the Emilia sequence. Preliminary analysis and model compatibility assessment. *Ann Geophys* 2012;2012:55.
- [37] Petti L, Lodato A. Preliminary spatial analysis and comparison between response spectra evaluated for Emilia Romagna earthquakes and elastic demand spectra according to the new seismic Italian code; 2012. <<http://www.reluis.it>>.
- [38] DM 14/01/2008. Nuove norme tecniche per le costruzioni. Ministero delle Infrastrutture (GU n. 29 04/02/2008), Rome, Italy [New technical norms on constructions].
- [39] Circolare n° 617 del 2 febbraio 2009. Istruzioni per l'applicazione delle nuove norme tecniche per le costruzioni di cui al decreto ministeriale 14 gennaio 2008 [Instructions for the application of the new technical norms on constructions].
- [40] Simulia. ABAQUS Theory Manual, USA; 2007.
- [41] Lubliner J, Oliver J, Oller S, Oñate E. A plastic-damage model for concrete. *Int J Solids Struct* 1989;25(3):299–326.
- [42] Labuz JF, Biolzi L. Characteristic strength of quasi-brittle materials. *Int J Solids Struct* 1998;35(31–32):4191–203.
- [43] Biolzi L, Pedalà S, Labuz JF. Mechanical characterization of natural building stone. *Geotechn Spec Publ* 1997;72:33–41.
- [44] Page AW. The biaxial compressive strength of brick masonry. *Proc Inst Civ Engrs* 1981;Part 2, 71(Sept):893–906.
- [45] Milani G, Lourenço PB, Tralli A. Homogenised limit analysis of masonry walls. Part II: structural examples. *Comput Struct* 2006;84:181–95.
- [46] Milani G, Lourenço PB, Tralli A. A homogenization approach for the limit analysis of out-of-plane loaded masonry walls. *J Struct Eng ASCE* 2006;132(10):1650–63.
- [47] Foraboschi P. Coupling effect between masonry spandrels and pier. *Mater Struct/Mater Constr* 2009;42(3):279–300.
- [48] Foraboschi P, Vanin A. Non-linear static analysis of masonry buildings based on a strut-and-tie modeling. *Soil Dyn Earthquake Eng* 2013;55:44–58.
- [49] Milani G, Valente M. Determination of the behavior factor of masonry churches by means of non-linear static and dynamic analyses; submitted for publication [2015].
- [50] Foraboschi P. Resisting system and failure modes of masonry domes. *Eng Fail Anal* 2014;44:315–37.
- [51] Minghini F, Milani G, Tralli A. Seismic risk assessment of a 50 m high masonry chimney using advanced analysis techniques. *Eng Struct* 2014;69:255–70.